© 2022. Published by The Company of Biologists Ltd | Journal of Cell Science (2022) 135, jcs260110. doi:10.1242/jcs.260110

RESEARCH ARTICLE

Reduction of nucleolar NOC1 leads to the accumulation of pre-rRNAs and induces Xrp1, affecting growth and resulting in cell competition

Francesca Destefanis[1,*], Valeria Manara[1,*], Stefania Santarelli[1,*], Sheri Zola[1], Marco Brambilla[2], Giacomo Viola[2], Paola Maragno[1], Ilaria Signoria[3], Gabriella Viero[3], Maria Enrica Pasini[2], Marianna Penzo[4,5] and Paola Bellosta[1,6,‡]

ABSTRACT

NOC1 is a nucleolar protein necessary in yeast for both transport and maturation of ribosomal subunits. Here, we show that *Drosophila* NOC1 (annotated CG7839) is necessary for rRNAs maturation and for a correct animal development. Its ubiquitous downregulation results in a dramatic decrease in polysome level and of protein synthesis. NOC1 expression in multiple organs, such as the prothoracic gland and the fat body, is necessary for their proper functioning. Reduction of NOC1 in epithelial cells from the imaginal discs results in clones that die by apoptosis, an event that is partially rescued in a *Minute*/+ background, suggesting that reduction of NOC1 induces the cells to become less fit and to acquire a 'loser' state. NOC1 downregulation activates the pro-apoptotic Eiger–JNK pathway and leads to an increase of Xrp1, which results in the upregulation of DILP8, a member of the insulin/relaxin-like family known to coordinate organ growth with animal development. Our data underline NOC1 as an essential gene in ribosome biogenesis and highlight its novel functions in the control of growth and cell competition.

KEY WORDS: *Drosophila*, NOC1, Eiger, DILP8, Xrp1, Cell competition, Apoptosis

INTRODUCTION

NOC1, NOC2 and NOC3 are members of a large family of conserved nucleolar proteins that play a critical role in the control of ribosome biogenesis in yeast and plants (Edskes et al., 1998; Li et al., 2009). Studies in *Saccharomyces cerevisiae* have revealed that NOC proteins are required for the maturation and processing of the rRNAs (Khoshnevis et al., 2019) and for transport of the pre-ribosomal 60S subunit in the cytoplasm through the formation of NOC1–NOC2 and NOC2–NOC3 heterodimers (Hierlmeier et al., 2013; Milkereit et al., 2001). NOC1–NOC3 have unique and essential roles, as mutation in each gene affects growth and viability in both *S. cerevisiae* and in *Arabidopsis* (Edskes et al., 1998; Li et al., 2009; Milkereit et al., 2001).

In *Drosophila*, efficient ribosome biogenesis is necessary during larval development, when increase in cell mass and animal size is highly dependent on protein synthesis (Texada et al., 2020). Mutations in genes that regulate this process, like those encoding for *Minute* family of ribosomal proteins (Marygold et al., 2007; Sæboe-Larssen et al., 1998) or for *Nop60b* (also known as *minifly* or *Dyskerin*) (Tortoriello et al., 2010) and *Nopp140* (Baral et al., 2020), components of the nucleolus, present similar defects that include a delay in development and reduced body size. Similar phenotypes have also been described for mutations in genes that control rRNA synthesis, such as the RNA-Pol-I associated chromatin regulator *PWP1* (Liu et al., 2017) or the *Rpl-135* subunit of the Pol-I complex (Grewal et al., 2005), and for *Myc* (Johnston et al., 1999), a master regulator of ribosome biogenesis both in *Drosophila* and in vertebrates (Barna et al., 2008; Destefanis et al., 2020; Grewal et al., 2005; van Riggelen et al., 2010).

Larval growth is also regulated by *Drosophila* insulin-like peptides DILPs (DILP2, DILP3 and DILP5; also known as ILP2, ILP3 and ILP5) released from the insulin-producing cells (IPCs) in response to nutrients (Géminard et al., 2009; Koyama et al., 2020; Maniere et al., 2020). This process is developmentally coordinated by the growth hormone ecdysone, secreted by the ring gland (Nijhout et al., 2014), and indirectly by DILP8, a peptide member of the Insulin/Relaxin family, secreted by cells from the peripheral organs in response to tissue damage (Garelli et al., 2015; Vallejo et al., 2015). The release of DILP8 (also known as ILP8), acting through the relaxin receptor Lgr3 in the brain, reduces the levels of ecdysone and delays development to ensure regeneration of the damaged tissues in coordination with the developmental timing (Boulan and Léopold, 2021). In cells of the imaginal discs, DILP8 upregulation has been associated with cell damage induced by the activation of the Eiger–JNK pathway (Sanchez et al., 2019), and more recently with the transcriptional upregulation of the Xrp1–RpS12 axis (Boulan and Léopold, 2021), which links signals of inter-organ coordination with proteotoxic stress. Indeed, reduced protein synthesis activates a stress response that triggers the activation of Xrp1, a pro-apoptotic CCAAT-enhancer-binding protein (C/EBP) transcription factor that, by reducing translation, activates the elimination of the unfit cells by cell competition (Baillon et al., 2018; Brown et al., 2021; Kiparaki et al., 2022; Langton et al., 2021). Mutations in ribosomal proteins, such as RpS3 (Akai et al., 2021; Baumgartner et al., 2021) and RpS12 (Ji et al., 2019; Lee et al., 2018), and the activation of the JNK/STAT signaling pathway (Kucinski et al., 2017), have been shown to control proteotoxic-induced cell competition, revealing how this process might by regulated by a complex network of signaling.

[1]Department of Cellular, Computational and Integrative Biology (CIBIO), University of Trento, Via Sommarive 9, 38123 Trento, Italy. [2]Department of Biosciences, University of Milano, Via Celoria 25, 20133 Milano, Italy. [3]Institute of Biophysics, CNR, Via Sommarive 18, 38123 Trento, Italy. [4]Department of Experimental, Diagnostic and Specialty Medicine, University of Bologna, Via Massarenti 9, 40138 Bologna, Italy. [5]Center for Applied Biomedical Research, University of Bologna, Via Massarenti 9, 40138 Bologna, Italy. [6]Department of Medicine, NYU Langone School of Medicine, 550 First Avenue, New York, 10016 NY, USA.
*These authors contributed equally to this work

‡Author for correspondence (paola.bellosta@unitn.it)

F.D., 0000-0003-2513-4622; V.M., 0000-0001-9292-6588; M.B., 0000-0002-4997-2404; G.V., 0000-0002-3502-9917; G.V., 0000-0002-6755-285X; M.P., 0000-0002-1738-9767; P.B., 0000-0003-1913-5661

Handling Editor: Maria Carmo-Fonseca
Received 8 April 2022; Accepted 25 October 2022

Journal of Cell Science (2022) 135, jcs260110. doi:10.1242/jcs.260110

In this study, we characterized the function of *Drosophila* nucleolar NOC1, NOC2 and NOC3 proteins (also known as CG7839, CG9246 and CG1234) *in vivo* and showed that their expression is necessary for proper animal growth. We demonstrate that NOC1 controls polysome abundance and its ubiquitous reduction blocks rRNA maturation resulting in reduced protein synthesis. In line with these results, lowering NOC1 levels in the whole animal results in small larvae that die early during development, whereas its reduction in different organs causes specific impairments of their function. In cells of the wing imaginal disc, NOC1 downregulation induces apoptosis that is partially rescued in a *Minute* (*M*)/+ background and by the expression of the baculovirus caspase inhibitor P35, a behavior that was typically described in loser cells and for genes that control cell competition. Our data identify that *NOC1-RNAi* cells show Xrp1 upregulation as well as activation of Eiger and JNK pathways, followed by an increase of DILP8 expression. However, DILP8 upregulation in our model is independent of Eiger expression, suggesting that Xrp1 may be inducing apoptosis in *NOC1-RNAi* by controlling specific pathways driven by proteotoxic stress.

RESULTS

Drosophila NOC1 localizes in the nucleolus and is necessary for animal growth

NOCs (for 'nucleolar complex associated') are members of a protein family characterized by the presence of a NOC domain, not conserved in all proteins, which is necessary for their heterodimerization (Milkereit et al., 2001). In *Drosophila*, the orthologs of yeast *Noc1*, *Noc2* and *Noc3* are annotated as *CG7839*, *CG9246* and *CG1234*, and are hereafter called *NOC1*, *NOC2* and *NOC3*. These genes, which are also present in humans, have a grade of conservation that varies from 32% to 35% identity within their amino acid sequences (Fig. 1A). Interestingly, a network analysis using the STRING database on predicted protein–protein interactions for NOC1/CG7839 uncovered that all three NOC proteins form a hub with other nucleolar proteins with a distinct role in ribosome biogenesis, suggesting that NOCs might function in concert to ensure proper nucleolar activity (Fig. S1).

Our results showed that ubiquitous reduction of NOC1, NOC2 or NOC3 in *Drosophila*, using RNA interference (RNAi) driven by the *actin* promoter resulted in small larvae that died between first and second instar (Fig. 1B, Table 1; Fig. S2A). Similar results were obtained upon CRISPR-Cas9-mediated homozygous mutation of *NOC1* (Fig. 1C; Fig. S3). By contrast, overexpression of NOC1 led to larvae that reached pupariation at almost the same size as the control but failed to maturate into adult animals. These data suggest that NOC1 is fundamental, and its expression must be tightly controlled to ensure proper animal development. These conclusions are supported by experiments that demonstrated that the co-expression of NOC1 in the RNAi animals compensates for NOC1 reduction, allowing larvae to develop (Fig. 1D,E) and to mature into small but viable adults (Fig. 1F–H). NOC1 has a unique function; indeed it does not complement NOC2 or NOC3 reduction since co-expression of NOC1 failed to rescue the lethality of NOC2-RNAi and NOC3-RNAi animals (data not shown). Next, we used the line CG7839-GFP.FPTB (modENCODE Model Organism ENCyclopedia Of DNA regulatory Elements), in which GFP-tagged NOC1 is expressed under the control of its regulatory sequences (Kudron et al., 2018), and showed that NOC1–GFP is expressed primarily in the nucleolus and colocalizes with fibrillarin in cells of the wing imaginal discs (Fig. 1I). The same result was confirmed in cells of the salivary glands, where the nucleolus is more evident (data not shown). Given that no commercial antibodies are available to characterize the endogenous protein, we expressed an HA-tagged form of NOC1 and determined its molecular mass as 132 kDa in lysates from 3rd instar larvae. In addition, we observed the presence of multiple bands at lower molecular masses detected with anti-HA antibodies (Fig. 1J), suggesting that NOC1 might undergo unusual proteolytic processes that might be linked to its toxicity observed in larvae at the pupae transition (Table 1). Overexpression of HA–NOC1 in the columnar epithelium of the wing imaginal discs using the *engrailed* promoter confirmed its colocalization with fibrillarin in the nucleolus (Fig. 1K,K′), this observation was better defined using the large cells of peripodium (Fig. 1M,M′). In addition, we noticed that, when overexpressed, NOC1 was included in large nuclear granules outside the nucleolar zone, clearly visible in the nuclei of peripodium cells (Fig. 1M,M′). These large structures and the abnormal nucleolar morphology were rescued when *NOC1-RNAi* was co-expressed with HA–NOC1 (Fig. 1L,L′,N,N′).

NOC1 is important for rRNA processing, ribosome maturation and functional protein synthesis

To investigate the role of *Drosophila* NOC proteins in ribosome biogenesis, we first analyzed the impact of NOC1 on ribosome maturation and protein synthesis. Polysome profiling in whole larvae showed that overexpression of NOC1 significantly increased the abundance of the 80S, and polysome peaks were increased compared to the wild type (WT) (Fig. 2A,B). By contrast, NOC1 reduction resulted in a dramatic decrease in ribosomal subunits and polysome abundance (Fig. 2C) with a robust reduction of the 80S and the relative increase of the 40S and 60S subunits, suggesting a defect in ribosome recruitment on polysomes (Fig. 2D,E). In yeast, the NOC1–NOC2 complex has been shown to regulate the activity of Rpr5, an assembly factor that blocks the cleavage of the internal transcribed spacers (ITS) during the rRNA precursors maturation, a process necessary for the stoichiometric production of the two ribosomal subunits (Khoshnevis et al., 2019). To assess whether *Drosophila* NOC1 also controlled this process, we quantified the levels of ITS1 and ITS2 and of the relative mature RNAs by qRT-PCR. This analysis showed that reduction of NOC1 induced the accumulation of the intermediate ITS1 and ITS2 immature forms of rRNAs with consequent reduction of the 18S and 28S rRNA levels (Fig. 2F). By contrast, NOC1 overexpression only reduced the level of ITS1 but not of ITS2, and significatively increased the amount of 18S and 28S rRNAs (Fig. 2F). These data confirm that NOC1 is also part of the mechanism that controls rRNAs synthesis and ribosomal processing in flies. To evaluate whether these defects reflected changes in global protein synthesis, we performed a surface sensing of translation (SUnSET) assay (Deliu et al., 2017). These experiments showed that in *NOC1-RNAi* animals, the translation of labeled puromycin peptides was robustly diminished compared to that seen in control animals (Fig. 2G–I). By contrast, overexpression of NOC1 did not significantly impair translation (data not shown).

Reduction of NOC1, NOC2 and NOC3 during development limits growth in the eye by affecting the number and size of the ommatidia but does affect the size in differentiated ommatidia

We then better characterized the role of NOCs *in vivo* by analyzing the impact of modulation of their expression in organs that represent models for the growth of the animal. We started with an analysis of NOCs in tissues with different proliferative characteristics. We used the *GMR* promoter (Hay et al., 1994) to modulate NOC expression at mid-third-instar stage in the differentiated cells of the retina, and the *tubulin* promoter in combination with *eyeless*-flippase, to restrain the

Journal of Cell Science (2022) 135, jcs260110. doi:10.1242/jcs.260110

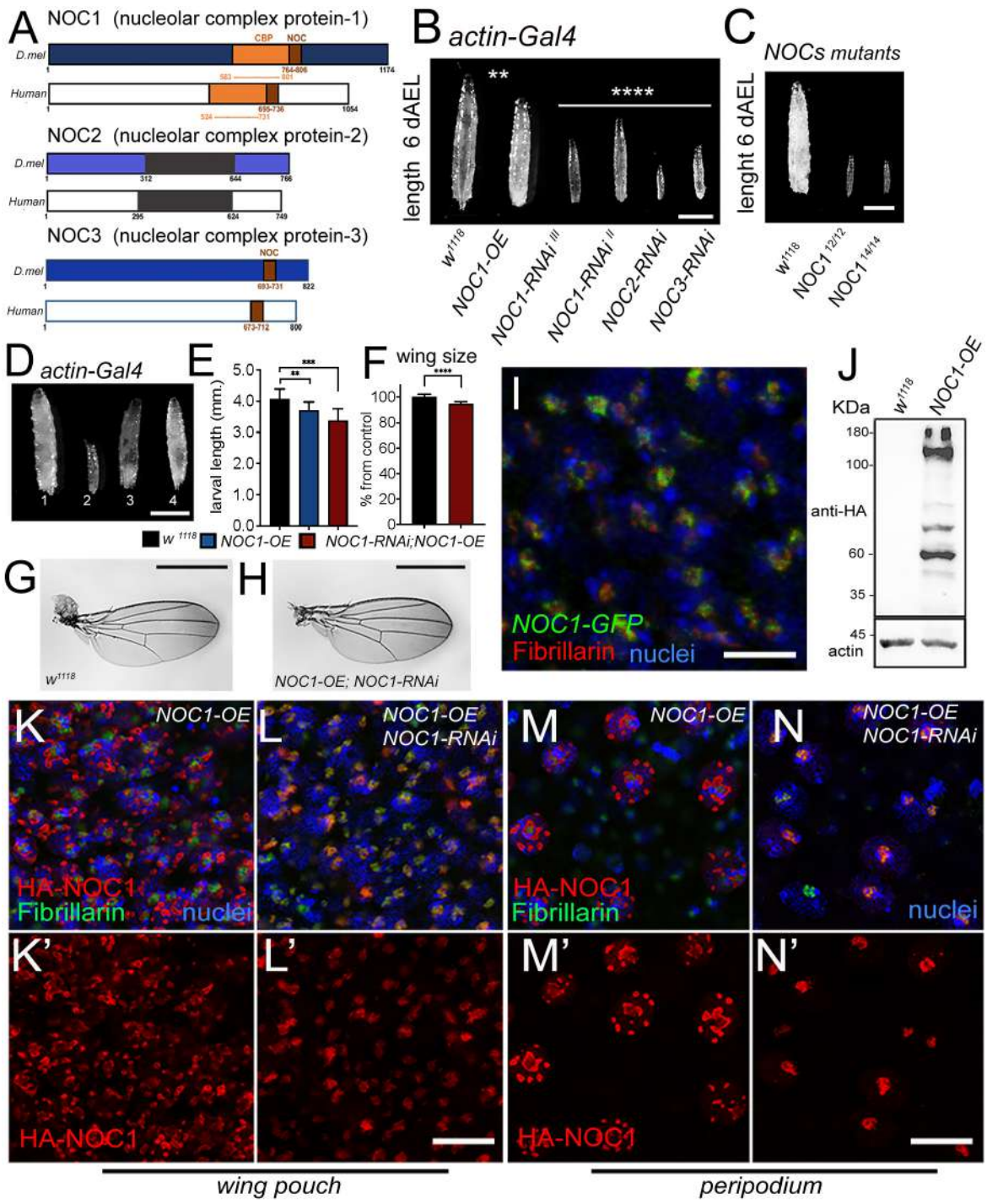

Fig. 1. See next page for legend.

expression of NOCs to the proliferative cells precursors of the eye and antenna discs (Bellosta et al., 2005). These experiments showed that downregulation of NOC1, NOC2 or NOC3 or NOC1 overexpression (OE) in differentiated cells driven by the *GMR* promoter did not affect the eye morphology nor their size (Fig. 3A–E; Fig. S4A). By contrast, downregulation of NOC1, NOC2 or NOC3 using the *tubulin* promoter, resulted in small eyes with smaller and disorganized ommatidia (Fig. 3H–J,N; Fig. S4B) whereas no defects were observed with NOC1 overexpression (Fig. 3G,N). Moreover, the growth defect induced by *NOC1-RNAi* was rescued by co-expression of the inhibitor of caspase P35 (Fig. 3L,M,O), indicating that the eye defects were the result of apoptosis.

Reduction of NOC1 in the prothoracic gland delays animal development by reducing ecdysone levels

The prothoracic gland (PG) produces the hormone ecdysone, which controls animal development (Nijhout et al., 2014). Reduction of NOC expression using the *P0206-Gal4* promoter has been previously shown to result in a delay in development (Valenza et al., 2018); these animals never pupariated and continued to grow

Journal of Cell Science (2022) 135, jcs260110. doi:10.1242/jcs.260110

Fig. 1. NOC1 is expressed in the nucleolus and its reduction, as for NOC2 and NOC3, affects animal growth and survival. (A) Schematic representation of *Drosophila* NOC1, NOC2 and NOC3 proteins and their human homologs, called CEBPz, NOC2L and NOC3L, respectively. NOC1 protein contains a CBP domain (CCAAT-binding domain), in orange, that shares 32% identity between sequences. The conserved NOC domain of 45 amino acids, present only in NOC1 and NOC3, is presented in brown; this shares 48% and 38% sequence identity between *Drosophila* and human proteins, respectively. NOC2 protein shares an overall 36% identity between *Drosophila* and human proteins; black represents the region of highest conservation (48%). (B) Photos of third-instar larvae expressing the indicated transgenes under the *actin* driver, taken at 120 h AEL. (C) Photos of control and $NOC1^{12}$ and $NOC1^{14}$ mutant third-instar larvae of 120 h AEL. (D) Photographs of larvae at 120 h AEL expressing the following transgenes (1) control w^{1118}, (2) *NOC1-RNAi*, (3) *NOC1* overexpression (OE), (4) *NOC1-RNAi; NOC1-OE* using the *actin-Gal4* driver. (E) Larval length measured in mm at 120 h AEL. (F) Quantification of wing area/size in animals of the indicated genotype; the number is expressed as mean±s.d. percentage of the control *actin-*w^{1118}, set at 100%. For E and F, at least 10 animals were used for each genotype; the experiment was repeated twice. (G-H) Photos representing wings from females of the indicated genotypes. (I) Confocal image of cells from the wing imaginal disc showing NOC1–GFP expression visualized using anti-GFP antibodies in green and anti-fibrillarin in red; nuclei are visualized with Hoechst. (J) Western blot from larval lysates expressing *HA-NOC1* under the *actin* promoter. A band of ∼130 kDa is the expected size for NOC1, is visualized by anti-HA antibody with a few other bands at lower molecular mass; actin is used as control loading. (K–N) Confocal pictures of cells from the wing imaginal discs (K,L) or from the peripodial epithelium (M,N) expressing *HA-NOC1* (K–M) or *HA-NOC1; NOC1-RNAi* (L,N) using the *engrailed* promoter. NOC1 expression was visualized using anti-HA antibodies in red and anti-fibrillarin in green. NOC1 expression alone is shown in K′–N′. ***P*<0.01; ****P*<0.001; *****P*<0.0001 [one-way ANOVA with Tukey multi-comparisons test (E); unpaired two-tailed Student's *t*-test (F)]. Images and blots shown are representative of three experiments. Scale bars: 1 mm (B–D,G,H); 5 µm (I), 10 µm (L,N).

for about 20 days (Table 1) increasing the size of the cells in the fat bodies (FB) (Fig. 4A,B) (Valenza et al., 2018). Macroscopic analysis of the PG in *NOC1-RNAi* animals did not reveal any morphological defects and, at 5 days after egg laying (AEL), their size was similar to that of control animals. However, at 12 days AEL the size of the PG in *NOC1-RNAi* animals was significantly atrophic (Fig. 4D–F). We next determined the levels of ecdysone by indirectly measuring the expression of its target mRNA *Ecdysone-induced protein 74b* (*E74b*; also known as *Eip74EF*). These data showed that *E74b* mRNA expression from whole larval tissues was already reduced at 5 days AEL in *NOC1-RNAi* animals compared to controls and it was further lowered at 12 days AEL (Fig. 4C). By contrast, NOC1 overexpression did not lead to any detectable changes in *E74b* mRNA level or in change in larval body size (data not shown).

NOC1 downregulation in the fat body reduces cell size and lipid storage resulting in dyslipidemia

Lowering NOC1, NOC2 or NOC3 expression in flip-out clones analyzed in the FB significantly reduced cell size and induced morphological defects (Fig. 5C–F). We then investigated the impact of reducing NOC1 in the whole organ using the *Cg* (*Collagen 4a1*; also known as *Col4a1*) (Parisi et al., 2013) and the promoter driving in the FB (denoted *FB*) (Schmid et al., 2014). These experiments showed that reduction of NOCs in the FB was lethal with similar results obtained using both promoters (Table 1). A deeper analysis using the *Cg* promoter showed that reduction of NOC1 delayed the time of larval development (> than 24 h). These animals are smaller when compared to control and eventually die between the late third-instar and at pupal stages (Fig. 5G, Table 1); only a small percentage of animals (<10%) hatched as small adults when we used *NOC1-RNAi* expressed on chromosome II (Fig. 5H), which was significantly less effective than the line on chromosome III in reducing *NOC1* mRNA levels (Fig. S5A). By contrast, overexpression of NOC1 increased larval volume, significantly at 96 AEL, resulting in adults that hatched with a slightly bigger size than control, as shown by analysis of their wing size (Fig. 5H). One function of the FB is to store lipids and sugars necessary for the animal to develop and to survive metamorphosis. Analysis of the contents of triglycerides (TGAs) showed that *NOC1-RNAi* larvae had less lipids compared to WT sibling animals taken at the same stage of development (Fig. 5I). A morphological analysis of the larval tissues using Nile Red to stain lipids, showed that the FB near the salivary glands (sg) was almost absent in *NOC1-RNAi* animals (Fig. 5J,N). Indeed, we observed that *NOC1-RNAi* animals accumulated a high level of lipids in the gut (Fig. 5K,O), in the brain and in the imaginal discs (Fig. 5L,P). This is a response to the reduced lipid storage capability of these animals, and represents induction of dyslipidemia, an inter-organ process that is active when fat cells fail to properly store lipids and non-autonomously stimulates other organs to accumulate them (Palm et al., 2012).

The FB also remotely controls the release of *Drosophila* insulin-like peptides (DILP2, DILP3 and DILP5) from the IPCs; these peptides are normally secreted in the hemolymph in response to nutrients but are retained when animals undergo starvation (Géminard et al., 2009). Analysis of DILP2 expression in the IPCs showed that, even in adequate nutrient conditions (FED), DILP2 was retained in the IPCs of animals with reduced NOC1 in the FB (Fig. 5M–Q), suggesting that these animals lost the ability to remotely control the release of DILPs, thus mimicking starvation, a condition in which DILPs would ordinarily be retained.

NOC1 reduction in cells of the wing imaginal disc results in cell death and induces cell competition that is partially rescued in a *Minute*/+ background

To assess the impact of NOCs on the growth of epithelial cells, we generated flip-out clones where the level of NOCs was either reduced or overexpressed and GFP was co-expressed as a cellular marker. Clones were induced at 48 h AEL and analysis of their size and number was performed between 72–90 h AEL in wing imaginal discs. This analysis showed that NOC1 overexpression did not significantly alter cell morphology or size, and clones developed at similar rate to control cells expressing only GFP (Fig. 6A,B,J). By contrast, downregulation of NOCs caused a significant reduction in the number and size of the clones, and the few that we found contained smaller cells with a morphology reminiscent of dying cells (Fig. 6C–E,J). Further analysis showed that *NOC1-RNAi* clones induced at 48 h AEL were not detected when analyzed at 90 h AEL (Fig. 6G,H), whereas control GFP clones reached the size of ∼120 cells/clone (Fig. 6F–H). Only when clones were induced at 72 AEL were we able to score a few *NOC1-RNAi* clones, which were still significantly smaller than control and partially rescued when the inhibitor of caspase P35 was co-expressed (Fig. 6K–M). The size of the *NOC1-RNAi* clones was overall 15% the size of WT GFP clones, set as 100% (Fig. 6I,K,L), and co-expression of P35 was able to partially rescue *NOC1-RNAi* clonal size up to 60% of WT (Fig. 6I,M). These results suggest that cells with reduced NOC1 might be eliminated by the neighboring cells through cell competition, a mechanism described in cells with mutations in the ribosomal proteins of the *Minute* family in which cells with reduced protein synthesis were killed and

Journal of Cell Science (2022) 135, jcs260110. doi:10.1242/jcs.260110

Table 1. Characterization of results of RNAi and overexpression of NOC proteins *in vivo* using different promoters

Tissue	Promoter (Gal4 driver)	Shown in figure	Transgene	Larval stage	Pupal stage	Adult
Whole body	*actin*	Fig. 1B,D	NOC1 OE	Viable	Lethal	–
			NOC1-RNAi	Lethal at L2, small	–	–
			NOC2-RNAi	Lethal at L2, small	–	–
			NOC3-RNAi	Lethal at L2, small	–	–
			NOC1RNAi; NOC1 OE	Viable, small size	Viable	Viable, small size
Neurons	*Elav*		NOC1 OE	Viable	Viable	Viable, no eye defects
			NOC1-RNAi	Delayed	Lethal	–
			NOC2-RNAi	Delayed	Lethal	–
			NOC3-RNAi	Delayed	Lethal	–
Retina	*GMR*	Fig. 3A–E	NOC1-RNAi	Viable	Viable	Viable, no eye defects
			NOC1-RNAi	Viable	Viable	Viable, no eye defects
			NOC2-RNAi	Viable	Viable	Viable, no eye defects
			NOC3-RNAi	Viable	Viable	Viable, no eye defects
Eyes and antenna	*tub-ey>flp*	Fig. 3F–J	NOC1 OE	Viable	Viable	Viable, no eye defects
			NOC1-RNAi	Viable	Viable	Viable, small eye, defects
			NOC2-RNAi	Viable	Viable	Viable, small eye, defects
			NOC3-RNAi	Viable	Viable	Viable, small eye, defects
PG	*P0206*	Fig. 4A	NOC1 OE	Viable	Viable	Viable, no defects
			NOC1-RNAi	Delayed, big larvae	No pupae	–
			NOC2-RNAi	Delayed, big larvae	No pupae	–
			NOC3-RNAi	Delayed, big larvae	No pupae	–
FB	*Cg*	Fig. 5G,H	NOC1 OE	Viable	Viable	increased body size
			NOC1-RNAi	Delayed, semi lethal at L3	Semi lethal, small	Lethal, few escapers*
			NOC2-RNAi	Delayed, lethal at L2/L3	Lethal, small pupae	–
			NOC3-RNAi	Delayed, lethal at L2/L3	Lethal, small pupae	–
FB	*FB*	Fig. 5G,H	NOC1 OE	Viable	Viable	Viable, body size (ND)
			NOC1-RNAi	Delayed, lethal at L3	small pupae, lethal	–
			NOC2-RNAi	Delayed, lethal at L3	small pupae, lethal	–
			NOC3-RNAi	Delayed, lethal at L3	small pupae, lethal	–
Wing	*MS1096*	Fig. 7D,E	NOC1 OE	Viable	Viable	Viable**
			NOC1-RNAi	Delayed	Viable	Viable, crumpled wings
			NOC2-RNAi	Delayed	Viable	Viable, crumpled wings
			NOC3-RNAi	Delayed	Viable	Viable, crumpled wings
Wing	*engrailed*	Fig. S3	NOC1 OE	Viable	Viable	Viable
			NOC1-RNAi	Delayed, lethal***	–	–
			NOC2-RNAi	Delayed, lethal	–	–
			NOC3-RNAi	Delayed, lethal	–	–
			NOC1-RNAi; NOC1 OE	Viable, rescue	Viable	Viable

*a few escapers are born with small body size using line on chromosome II; **a few males are born with wing defects being *MS1096* in on chromosome X; ***immature imaginal discs are visible in NOC1-RNAi larvae using a transgene on chromosome II, whereas fewer imaginal discs are found using the RNAi line on chromosome III. OE, overexpression.

outcompeted by the WT neighboring cells (Baker, 2020). To understand whether *NOC1-RNAi* was triggering cell competition, we induced *NOC1-RNAi* clones in animals heterozygotes for the *Minute(3)66D* gene, which carries a mutation in the gene encoding for the ribosomal protein RpL14 (Sæboe-Larssen et al., 1997). These experiments showed that *NOC1-RNAi* clones were partially rescued in their number and size when induced in a *Minute* heterozygous background (Fig. 6N,O), suggesting that NOC1 is part of the mechanisms regulating ribosomal protein-induced cell competition.

Reduction of NOC1 induces the Eiger–JNK pathway, resulting in apoptosis and DILP8 upregulation, which depends on XRP1 activation

We further characterized the mechanisms underlining *NOC1-RNAi*-induced apoptosis in epithelial cells of the wing imaginal discs. We

Journal of Cell Science (2022) 135, jcs260110. doi:10.1242/jcs.260110

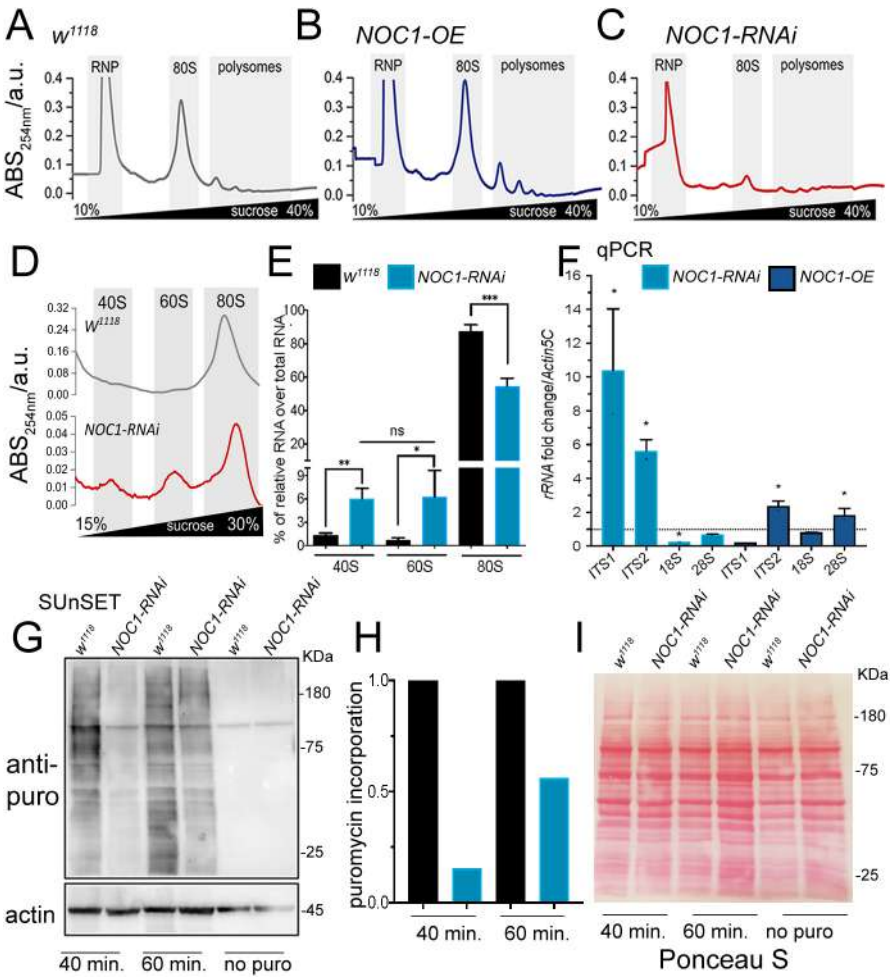

Fig. 2. NOC1 regulates rRNA processing and ribosomal assembling, affecting protein synthesis. (A–C) Representative sucrose density gradient profiles of ribosomes from control larvae (A) or animals over-expressing *NOC1* (B) or *NOC1-RNAi* (C). (D) More detailed view of results shown in A and C highlighting the area of the 40, 60 and 80S ribosomal subunits, noting that the graphs use different scales. (E) Analysis of the percentage of 40, 60 and 80S ribosomal subunits, relative to each genotype, calculated over the total area including the polysome. (F) qRT-PCR showing the fold of induction over control w^{1118} of pre-rRNAs analyzed using the ITSs and of mature ribosomal rRNAs; data are expressed relative to *actin5C* used as control. Results in E and F presented as mean±s.d. for at least three independent experiments. (G) SUnSET western blot analysis of lysates from larvae treated with puromycin for the indicated time. The blot shows the relative changes in protein synthesis using anti-puromycin antibodies in control w^{1118} or in larvae ubiquitously expressing *NOC1-RNAi* under the *actin* promoter. Actin was used as control loading. (H) Quantification of the change in puromycin incorporation from G and normalized relative to actin (Deliu et al., 2017). Results show mean from two experiments. (I) Ponceau S staining showing total protein levels in G. **P*<0.05; ***P*<0.01; ****P*<0.001; ns, not significant (one-way ANOVA with Tukey multi-comparisons test). Images and blots shown are representative of two experiments.

started this analysis using the *MS1096* dorsal wing promoter (Capdevila and Guerrero, 1994) and showed that both overexpression of NOC1 and its reduction did not significantly affect the morphology of the discs, which exhibited the correct pattern for Wingless expression (Fig. 7A–C). However, when we analyzed the timing of larval development, we observed that *NOC1-RNAi* animals developed to a smaller size than control with a significant difference at 120 h AEL (Fig. 7D). These larvae were delayed in their development and reached pupariation 24 h late with respect to larvae from control or *NOC1-OE* animals (Fig. 7E; Table 1). In addition, reduction of NOC1 using the RNAi line on chromosome III resulted in pupal lethality, while using the line on chromosome II resulted in <10% of animals hatching with wings that presented morphological defects in the dorsal side and were significantly smaller (Fig. 7F–H; Fig. S5B). The combination of developmental delay and apoptosis prompted us to check whether the reduction of NOC1 upregulates DILP8, which is normally secreted in response to cell death and tissue damage. Indeed, we found *Dilp8* mRNA levels significantly increased (>40×) in these larvae (P<0.01), whereas its level was not changed upon NOC1 overexpression (data not shown).

To better analyze at cellular level the mechanism underlying DILP8 upregulation, we reduced NOC1 using the wing-specific *rotund* (*rn*)-*Gal4* promoter. These experiments confirmed that in cells where NOC1 was reduced, the level of DILP8–GFP increased (Fig. 7I,J) (similar results were obtained using the *MS1096* promoter; data not shown). We also found an upregulation of the pro-apoptotic gene *eiger* using its reporter *eiger-GFP* in *NOC1-RNAi* cells (Fig. 7N,O), which was accompanied by an activation of JNK signaling indicated by the increase in *TRE-dsRED* (Fig. 7R,S). In agreement with these results, anti-Caspase3 staining indicated that apoptosis was significantly increased in cells with reduced NOC1 (Fig. 7V,W). Cells undergoing proteotoxic stress are subjected to elimination by cell competition through a mechanism that depends on Xrp1, a transcription factor upregulated in cells heterozygous for Ribosomal proteins ($Rp^{+/-}$) (Lee et al., 2018). Notably, we found that *NOC1-RNAi* cells transcriptionally upregulated Xrp1, as analyzed using the $Xrp1^{02515}$-*LacZ* reporter line (Baillon et al., 2018) (Fig. S6). These data strongly suggest that cells with reduced NOC1 undergo proteotoxic stress with upregulation of *Xrp1* and *eiger*, causing cell damage that activates the DILP8/Lgr3 compensatory mechanism, responsible for the developmental delay observed in *NOC1-RNAi* animals. We then performed epistasis experiments to better determine the roles of Xrp1 and Eiger in activating the DILP8 response. Unfortunately, the contemporary reduction of NOC1 and Xrp1 using either *rotund* or *nubbin* promoters resulted in embryonic lethality, whereas larvae with both NOC1 and Eiger downregulation using the same promoters were viable. Using *nubbin*-Gal4, we then analyzed whether DILP8 upregulation was Eiger dependent. These experiments demonstrate that the NOC1-RNAi-induced DILP8 upregulation, even if partially reduced, was not significantly dependent on Eiger expression, using DILP8–GFP quantification (Fig. 7K,L,P,Q,M). These data were also confirmed by qRT-PCR of

Journal of Cell Science (2022) 135, jcs260110. doi:10.1242/jcs.260110

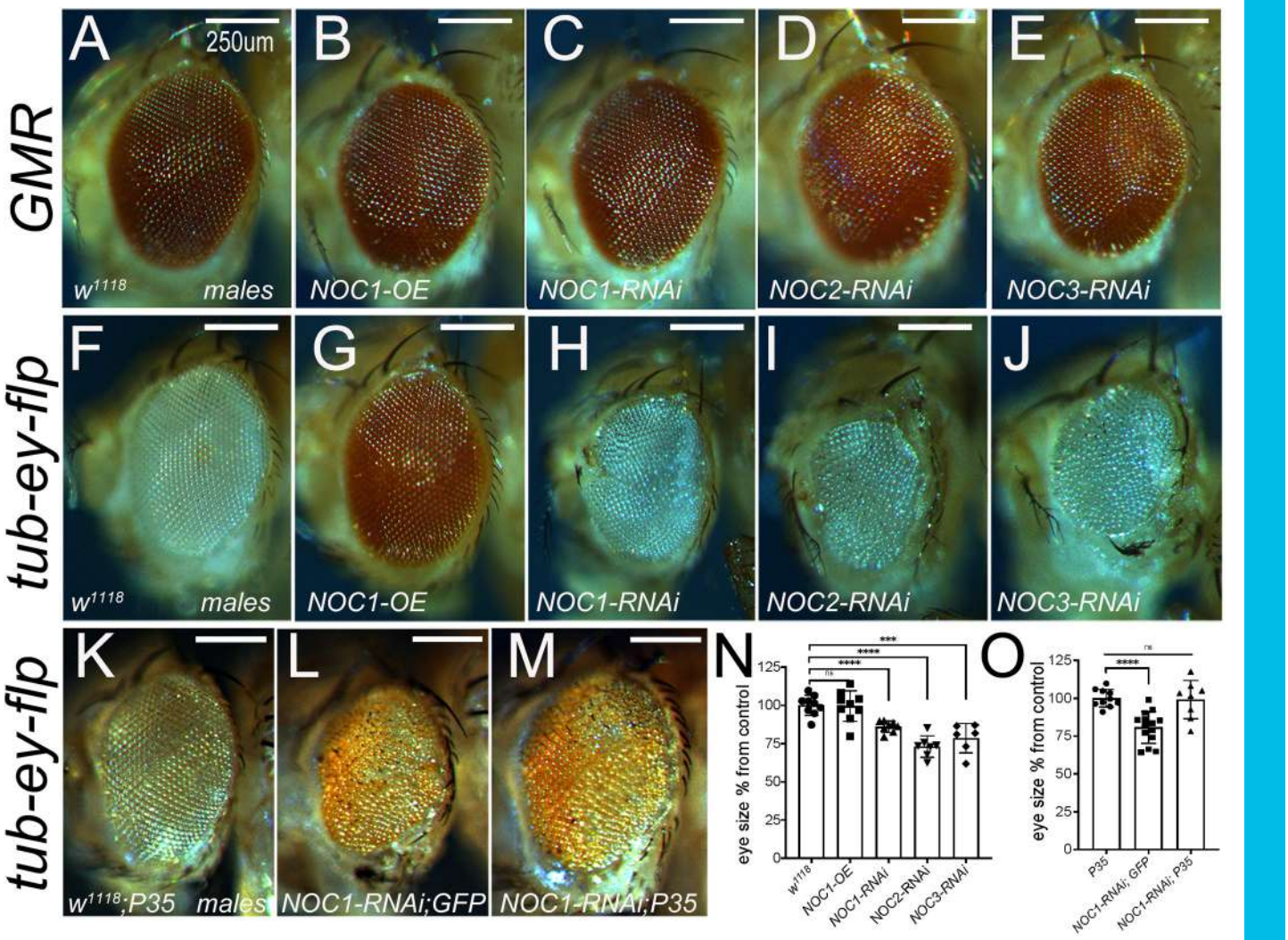

Fig. 3. Reduction of NOC1, NOC2 and NOC3 during development affects the number and size of the ommatidia by inducing apoptosis but does not affect the differentiated ommatidia. Photographs of *Drosophila* compound eyes (lateral view) expressing the indicated transgenes using the *GMR-Gal4* promoter (A–E) or the *tubulin-GAl4* promoter in combination with *eyeless-flippase* to constrain Gal4 expression to the proliferative cells of the eye and antenna (F–J) (Bellosta et al., 2005). (K–M) Photographs of compound eyes expressing the caspase inhibitor *P35* alone (K) or together with *NOC1-RNAi* (M) that rescues the eye defect showed in L. Photographs were acquired from male's eyes and similar data were obtained using females (not shown). (N,O) Quantification of eye size from F–J (N) and from K–M (O); values are expressed as the mean±s.d. percentage of control, set at 100% (*n*=10). ***P<0.001; ****P<0.0001; n.s., not significant (unpaired two-tailed Student's *t*-test). Scale bars: 250 µm.

Dilp8 mRNA, which was not significantly changed when the *eiger* level was reduced by RNAi (Fig. 7T; Fig. S7). Moreover, *Xrp1* mRNA levels, which are increased upon NOC1 downregulation, are not reduced in imaginal discs from *NOC1-RNAi; eiger-RNAi* animals (Fig. 7U). Overall, these results suggest that DILP8 expression is predominantly controlled by Xrp1 and point to a more upstream role for Xrp1 in respect to Eiger in controlling the proteotoxic response following reduction of NOC1 (Fig. 7X).

DISCUSSION

We have shown that the *Drosophila* homologs of yeast NOC1, NOC2 and NOC3 (Fig. 1A) are required for animal development and their ubiquitous reduction results in growth impairment and larval lethality (Fig. 1B and Table 1). Ubiquitous overexpression of NOC1 is also detrimental but at the pupal stage, a phenotype that is rescued by co-expression of *NOC1-RNAi*, which allows the animals to develop to small adults (Fig. 1C–E). These data suggest that NOC1 expression must be tightly regulated, as either its reduction or overexpression may be detrimental for the cells. As demonstrated in yeast, the function of *Drosophila* NOC1 is not redundant with the other NOC proteins, and its overexpression does not compensate for the loss of *NOC2* and *NOC3* (data not shown). The reason for this behavior might be because NOC proteins function as heterodimers (NOC1–NOC2 and NOC2–NOC3) that are necessary for proper control of rRNA processing and the assembling of the 60S ribosomal subunits (Edskes et al., 1998; Hierlmeier et al., 2013; Milkereit et al., 2001). Indeed, it has been demonstrated in yeast that the NOC1–NOC2 complex regulates the activity of ribosomal RNA protein-5 (Rpr5), which controls rRNA cleavage at the internal transcribed spacers ITS1 and ITS2 sequences to ensure the stoichiometric maturation of the 40S and 60S ribosomal subunits (Khoshnevis et al., 2019). This function is likely to be conserved also in flies. In fact, our results show that reduction of NOC1 induces the accumulation of the intermediate ITS1 and ITS2 immature forms of rRNAs. Moreover, we observed a reduction in the relative abundance of 18S and 28S rRNAs (Fig. 2F), suggesting

Journal of Cell Science (2022) 135, jcs260110. doi:10.1242/jcs.260110

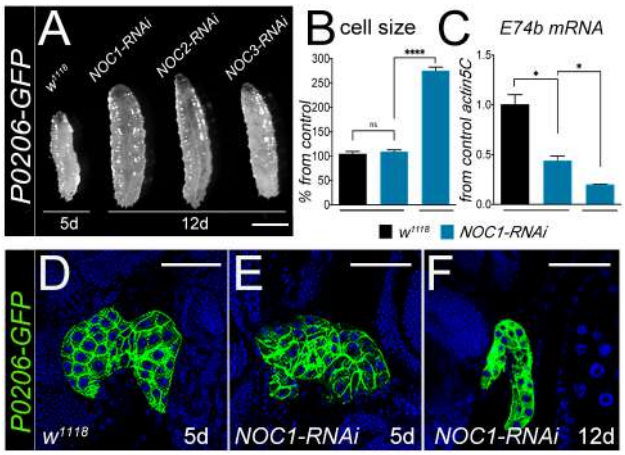

Fig. 4. NOC1 downregulation in the PG reduces ecdysone production and delays development. (A) Photographs of whole larvae with reduced NOC expression in the PG, driven by the *P0206* promoter. Picture represents w^{1118} larvae at 5 days AEL and *NOC1-RNAi*, *NOC2-RNAi* and *NOC3-RNAi* larvae at 12 days AEL. (B) Analysis (mean±s.d.) of the size in cells of the FB from control w^{1118} or *NOC1-RNAi* larvae at 5 days and at 12 days AEL. (C) qRT-PCR showing the level of *E74b* mRNA, target of ecdysone, from whole larvae at the indicated time of development. For B and C, more than 10 animals were used in each experiment from at least two independent experiments. (D–F) Confocal images of the ring gland marked with GFP, using the *P0206-GFP* driver line, from control w^{1118} (D) and from animals with reduced *NOC1* at 5 days AEL (E) and 12 days AEL (F). Nuclei are stained with Hoechst. **P*<0.05; *****P*<0.0001; n.s., not significant (one-way ANOVA with Tukey multi-comparisons test). Images shown are representative of one out of at least three experiments. Scale bars: 1 mm (A); 50 µm (D–F).

that NOC1 is also required in flies for proper rRNA processing and ribosome maturation (Milkereit et al., 2001). In line with this hypothesis, we demonstrated that NOC1 reduction results in a strong decrease in ribosome abundance and assembling, which is also accompanied by a strong reduction of the 80S and the polysomes (Fig. 2C). In addition, we also observed a mild accumulation of the 40S and 60S subunits (Fig. 2D,E), suggesting that the mature 80S ribosome might be unstable in *NOC1-RNAi* animals and that a small percentage of the ribosome disassembles into the two subunits, leading to the observed increase. In addition, given that NOC1 was identified as a predicted transcription factor (Kudron et al., 2018; Neumuller et al., 2013; Port et al., 2020), and because reduction of NOC1 results in a robust decrease in global protein synthesis (Fig. 2G,H), we cannot exclude that specific factors involved in the 80S assembling are reduced or missing in *NOC1-RNAi* animals.

Analysis of protein–protein interaction using STRING indicates that CG7838/NOC1 might act in a complex with other nucleolar proteins (Fig. S1). Indeed, here we showed that NOC1 colocalizes in the nucleolus with fibrillarin (Fig. 1I,K,M). Moreover, NOC1 overexpression also results in the formation of large round nuclear structures, which are significantly reduced when its expression is decreased by *NOC1-RNAi* (Fig. 1K′–L′,M′-N′). Interestingly, similar structures have been shown for CEBPz, the human homolog of NOC1, as visible in images from 'The Human Protein Atlas' (see https://www.proteinatlas.org/ENSG00000115816-CEBPZ/subcellular#img). CEBPz (also called CBF2 and CTF2; OMIM-612828) is a transcription factor member of the CAAT-binding protein family, which are involved in Hsp70 complex activation (Lum et al., 1990) and are upregulated in tumors, particularly in cells from patients with acute myeloid leukemia (AML) (Herold et al., 2014). As NOC1 also has the conserved CBP domain (Fig. 1A), this suggests that it might also act as a transcription factor, a hypothesis corroborated by data in *Drosophila* (CHIP-Seq and genetic screens) that demonstrates how its expression is associated to promoter regions of genes with a function in the regulation of nucleolar activity and of ribosomal proteins (Neumuller et al., 2013; Shokri et al., 2019). This observation is important as it opens up the possibility that NOC1 can control ribosome biogenesis through alternative mechanisms in addition to its control over rRNA transport and maturation. Moreover, we believe this function might be conserved for CEBPz, because in our bioinformatic analysis we identified nucleolar components and ribosomal proteins as being upregulated in liver and breast tumors with an overexpression of CEBPz (Table S1). Interestingly, misexpression of some of these targets, like Rpl5 and Rpl35a, have been associated with ribosomopathies, suggesting that mutations in CEBPz could contribute to tumorigenesis in these genetic diseases (Mills and Green, 2017; Narla and Ebert, 2010).

To better characterize NOC1 functions *in vivo*, we modulated its expression in organs that are relevant for *Drosophila* physiology, such as the prothoracic gland (PG), the FB and the wing imaginal discs.

Prothoracic gland

Although the overexpression of NOC1 in the PG does not affect development, its reduction significantly decreased ecdysone production, as shown by *E74b* mRNA levels (Fig. 4C). This reduction is significant both at 5 and at 12 days AEL, and occurs concomitantly with the reduction of the PG size (Fig. 4F). Consequently, *NOC1-RNAi* animals are developmentally delayed and do not undergo pupariation but rather continue to wander until they die at ∼20 days AEL (Fig. 4A). These animals feed constantly and increase their size, accumulating fats and sugars in the FB cells, which augment their size (Fig. 4B). We previously described the presence of hemocytes (macrophage-like cells) infiltrating the FB of these animals, a condition accompanied with an increase in JNK signaling and reactive oxygen species (ROS), likely released by the fat cells under stress conditions (Valenza et al., 2018). Interestingly, this intercellular event recapitulates the chronic low-grade inflammation, or adipocyte tissue macrophage (ATM), a pathology associated with adipose tissue in obese people that represents the consequence of impaired lipid metabolism (Horng and Hotamisligil, 2011).

Fat body

Reduction of NOC1, NOC2 or NOC3 in the FB results in smaller and fewer cells (Fig. 5C–F), whereas reduction of NOC1 in the whole organ inhibits animal development (Table 1). The FB regulates animal growth by sensing amino acids concentrations in the hemolymph and remotely controlling the release of DILP2, DILP3 and DILP5 from the IPCs (Andersen et al., 2013; Géminard et al., 2009; Hyun, 2018). The FB also stores the nutrients (fats and sugars) that are necessary during the catabolic process of autophagy to allow animals to survive metamorphosis (Rusten et al., 2004; Scott et al., 2004). When nutrients are limited, larvae delay their development to accumulate fats and sugars until reaching their critical size, which ensures they can progress through metamorphosis (Hironaka et al., 2019; Texada et al., 2020). NOC1 downregulation in the FB alters its ability to store nutrients, and larvae proceed poorly through development (Fig. 5G). In addition, these animals show DILP2 accumulation in the IPCs even in normal feeding conditions (Fig. 5Q), indicating that the remote signals responsible for DILP release are greatly reduced, phenocopying

Journal of Cell Science (2022) 135, jcs260110. doi:10.1242/jcs.260110

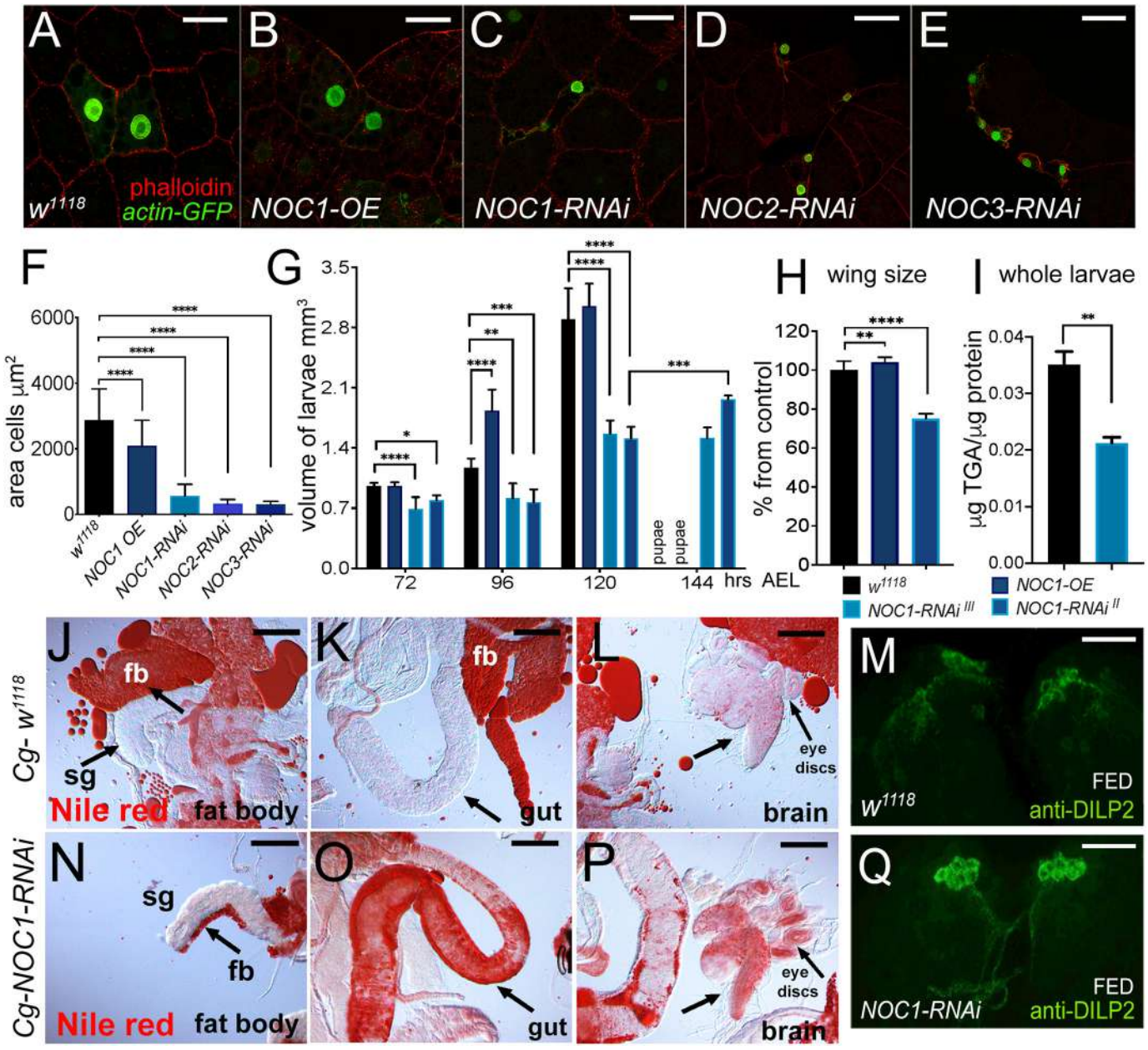

Fig. 5. NOC1 downregulation in the FB reduces its size and TGA content resulting in larval lethality and induces dyslipidemia. (A–E) Confocal images of *actin*-flip-out clones in the FB co-expressing nuclear GFP together with the indicated transgenes. Phalloidin–Texas Red was used to mark cell membranes. (F) Quantification (mean±s.d.) of the size of the cells in the clones from the FB; data are from at least two independent experiments. (G) Analysis of larval volume measured at the indicated time of development until pupariation in animals in which the NOC transgenes were expressed using the *Cg* promoter. Data show one of three experiments using ten or more animals for each genotype. (H) Analysis of the wing size from 4-day-old female adult flies of the indicated genotypes, data are expressed as mean±s.d. percentage from control w^{1118}. (I) Quantification mean±s.d. of triglyceride (TGA) levels in whole larvae at 120 h AEL, data are expressed as microgram of TGAs per microgram of proteins. Data in G–I are from at least two independent experiments. (J–L,N–P) Photographs of larval organs stained with Nile Red to visualized lipids from control w^{1118} (J–L) and *NOC1-RNAi* animals (N–P) at third instar. Reduction of *NOC1-RNAi* affects the size of the FB (fb) particularly visible near the salivary gland (sg indicated by the arrow). The impairment to accumulation of nutrients in the FB in *NOC1-RNAi* animals induces the storage of fats in other organs, visible in the gut, as indicated by the arrow in K and O, and in the brain and eye imaginal discs, indicated by the arrow in L and P. (M,Q) Confocal images of third-instar larval brains showing DILP2 immunostaining in the IPCs from control w^{1118} (M) and *NOC1-RNAi* (Q) animals in feeding conditions. *P<0.05; **P<0.01; ***P<0.001; ****P<0.0001 [one-way ANOVA with Tukey multi-comparisons test (F–H); Student's *t*-test (I)]. Images shown are representative of one out of at least three experiments. Scale bars: 50 µm (A–E,M,Q); 100 µm (J–L,N–P).

animals in starvation or with reduced levels of MYC in fat cells (Géminard et al., 2009; Parisi et al., 2013). Interestingly, we also observed that *Cg-NOC1-RNAi* animals accumulate an abnormal amount of fats in non-metabolic organs, such as gut, brain and imaginal discs (Fig. 5O,P). This finding suggests that these animals are subjected to inter-organ dyslipidemia, a mechanism of lipid transport activated when the FB function is impaired, which triggers non-autonomous signals to induce other organs to store fats. Interestingly, this condition recapitulates dyslipidemia in humans, where the compromised adipose tissue releases lipoproteins of the APO family,

Journal of Cell Science (2022) 135, jcs260110. doi:10.1242/jcs.260110

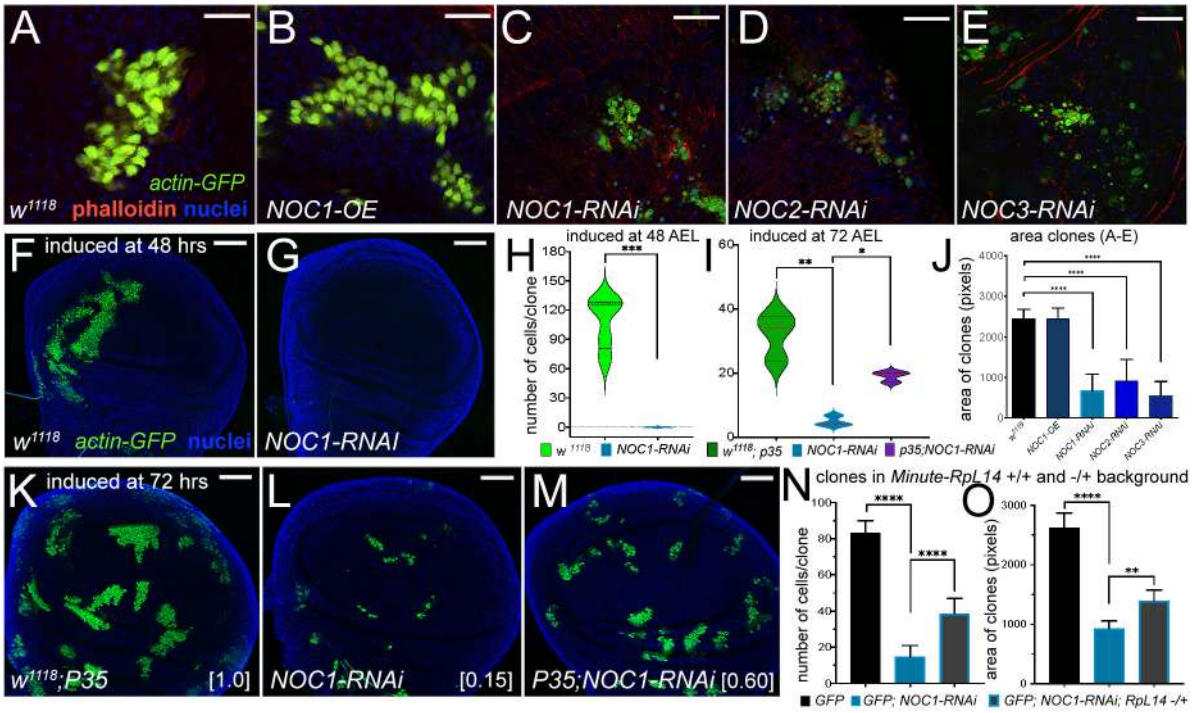

Fig. 6. Reduction of NOC1, NOC2 and NOC3 in cells of the wing imaginal disc induces growth defects that are rescued by co-expressing P35 and in a *Minute(3)66D*/+ heterozygous background. (A–E) Confocal images of *actin*-flip-out clones analyzed in the wing imaginal discs, expressing nuclear GFP and the indicated transgenes. Phalloidin–Texas Red was used to mark the cell membranes (red) and Hoechst for the nuclei (blue). (J) Quantification of clonal size performed by measuring the area marked by phalloidin; area is shown in pixels (mean±s.d.). At least 15 animals from each genotype were used. (F,G) Confocal images of wing imaginal discs showing *actin*-flip-out clones expressing GFP alone (F) or co-expressing *NOC1-RNAi* (G). Clones were induced at 48 h AEL. (H,I) Quantification of the number of cells in each clone was analyzed at 120 h AEL using GFP as marker presented as violin plots with median and interquartile range marked by dashed lines. (K–M) Photographs of *actin*-flip-out clones in wing discs expressing GFP along with the inhibitor of caspase P35 (K), or with *NOC1-RNAi* (L) or co-expressing *NOC1-RNAi* together with P35 (M); clones were induced at 72 h AEL. The number of cells in each clone from K, L and M was quantified at 120 h AEL. The total number of clones analyzed in this experiment is: w^{1118}+P35 (72), *NOC1-RNAi* alone (66), and *NOC1-RNAi*+p35 (81). The numbers in square brackets represent the relative size of clones (average) compared to that from control considered equal to 1. (N,O) Analysis of cell number and clonal size of *NOC1-RNAi* clones induced in ribosomal protein $(Rp)^{+/-}$ and an Rp+/+ background using the *Minute(3)66D*/+ line that carries a mutation in the Rpl14 protein. (N) Quantification (mean±s.d.) of the number of clones in each disc. (O) Clonal size (mean±s.d.) showing that defects of *NOC1-RNAi* cells are partially rescued when clones are grown in the *Minute(3)66D*/+ ($Rp^{+/-}$) background. *P<0.05, **P<0.01, ***P<0.001 and ****P<0.0001 [unpaired two-tailed Student's *t*-test (H); one-way ANOVA with Tukey multiple comparisons (I,J,N,O)]. In F,G,K–M, Hoechst was used for staining the nuclei. Scale bars: 20 µm (A–E); 50 µm (F,G,K–M).

inducing fat accumulation in organs (Pirillo et al., 2021). Notably, a similar condition has also been described in flies for mutations in members of the *APOE* family (Palm et al., 2012), outlining how the mechanisms controlling the inter-organ fat metabolism are conserved among species.

Wing imaginal discs

NOC1 depletion in clones analyzed in the wing imaginal discs triggers their elimination by apoptosis (Fig. 6K–M). This event is partially rescued when clones are induced in the hypomorphic background of the *Minute(3)66D*/+ mutation (Sæboe-Larssen et al., 1997) (Fig. 6N,O). These cells also upregulate the pro-apoptotic gene *Xrp1* (Fig. 7U and Fig. S6), recently shown to be responsible for controlling translation and indirectly cell competition upon proteotoxic stress (Baillon et al., 2018; Baumgartner et al., 2021; Kiparaki et al., 2022). Reduction of NOC1 in the wing imaginal disc prolongs larval development (Fig. 7D,E) with upregulation of DILP8 (Fig. 7I–M) normally induced by cellular damage and apoptosis. The fact that *NOC1-RNAi* cells upregulate, in addition to Xrp1, *eiger* (Fig. 7N,O), another pro-apoptotic gene and member of the TNFα family, and activate the JNK pathway (Fig. 7R,S), suggests that different mechanisms are converging in these cells to induce apoptosis and DILP8 upregulation. We performed genetic epistasis experiments to define the relationship between Eiger signaling in *NOC1-RNAi* cells and how this is linked to Xrp1 transcriptional upregulation in response to nucleolar stress and DILP8 upregulation. This analysis showed that reduction of Eiger did not significantly affect DILP8 expression induced upon NOC1 downregulation (Fig. 7L–Q). Owing to the embryonic lethality induced by the simultaneous reduction of NOC1 and Xrp1 in cells of the wing imaginal discs, using both *rotund* and *nubbin* promoters, we analyzed the contribute of Eiger to Xrp1 and DILP8 transcriptional regulation upon *NOC1-RNAi*. These data indicate that DILP8 upregulation was not significantly affected by the reduction of Eiger seen upon NOC1 reduction (Fig. 7T), confirming the data *in vivo* with DILP8–GFP. In addition, we can predict that Xrp1 acts independently of Eiger, since *Xrp1* mRNA upregulation is not rescued in imaginal discs from *NOC1-RNAi*; *eiger-RNAi* animals (Fig. 7U), pointing out to a more upstream role for Xrp1 in controlling the stress response following reduction of NOC1; the function of Eiger remains to be determined.

In conclusion, our data corroborate the role of NOC1 in mechanisms that induce proteotoxic stress adding NOC1 as a novel component that links defects in protein synthesis with cell

Journal of Cell Science (2022) 135, jcs260110. doi:10.1242/jcs.260110

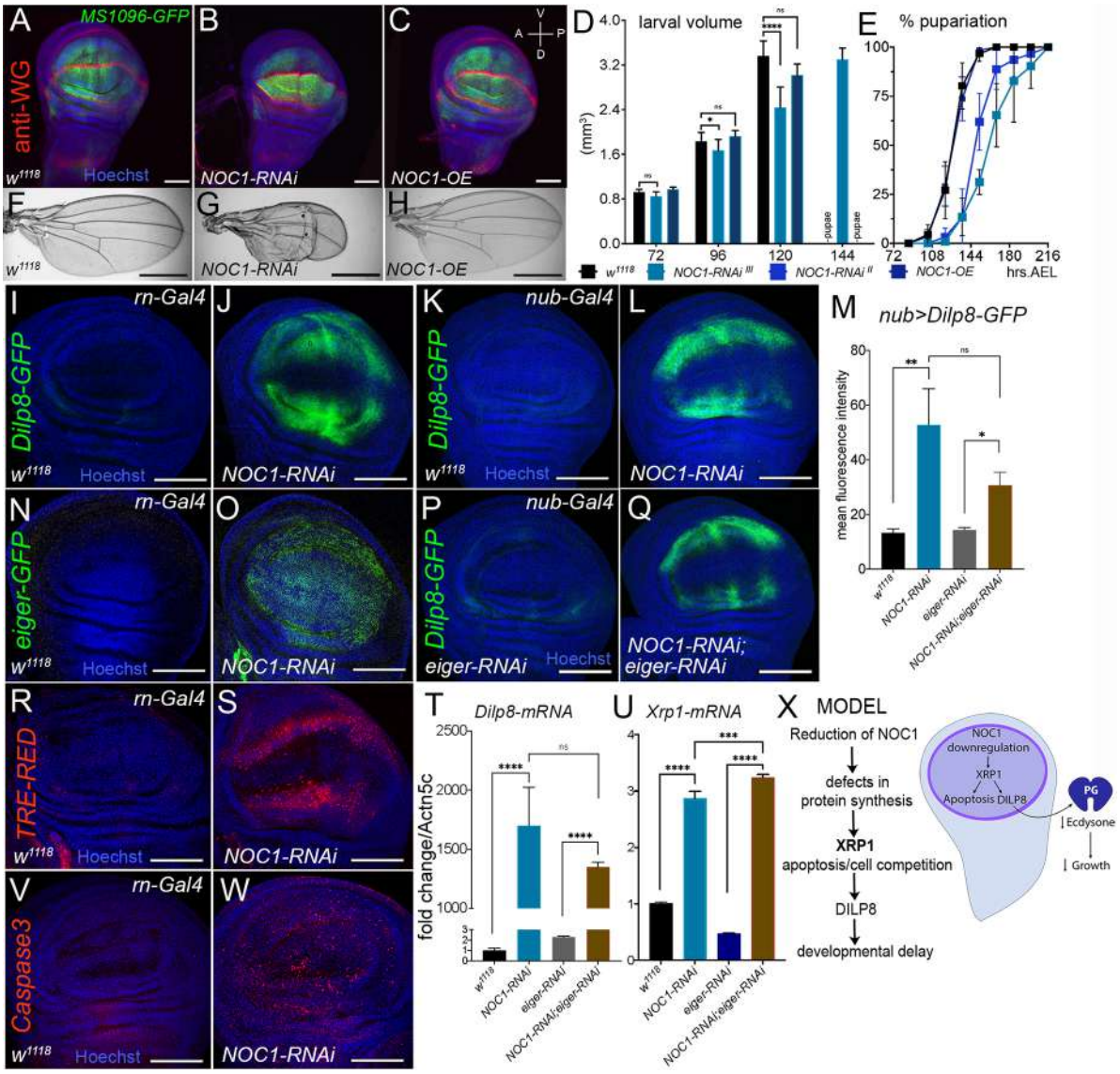

Fig. 7. Reduction of NOC1 in cells of the wing imaginal disc induces Xrp1 and Eiger resulting in apoptosis and DILP8-induced developmental delay. (A–C) Confocal images of wing imaginal discs expressing the indicated transgenes using the *MS1096-GFP* wing-driver. Wingless (WG) expression is visualized using anti-WG antibodies (in red), nuclei are stained with Hoechst (in blue). (D) Larval volume of animals expressing the indicated transgenes using the *MS1096*-driver was measured at the indicated time AEL until pupariation. The graph is the mean±s.d. for one of three experiments using at least ten animals for each point and genotype. (E) Curves representing the mean±s.d. percentage of larvae that underwent pupariation for the indicated genotypes. A significant delay in pupariation (one-way ANOVA with Tukey's test, $P<0.0001$) is visible in animals in which *NOC1* is reduced using *MS1096-Gal4* with both the RNAi lines. Data are expressed as percentage of pupariation over the total number of pupae of the same genotype, and are from five independent experiments. (F–H) Photographs of wings from 3-day-old adults of the indicated genotype. (I–W) Confocal images of wing imaginal discs from third-instar larvae where *NOC1-RNAi* was expressed using *rotund-Gal4* driver, co-expressing *DILP8-GFP* (I,J), *eiger-GFP* (N,O) or TRE-dsRED (R,S) reporters, or were stained for apoptotic cells using the anti-Caspase-3 antibody (V,W). (K–Q) Confocal images of wing imaginal discs expressing *NOC1-RNAi* using the *nubbin-Gal4* driver (K,L) or together with *eiger-RNAi* (P,Q), along with the DILP8–GFP reporter. (M) Quantification of the mean±s.d. GFP intensity in the wing pouch from K,L,O,P. (T,U) qRT-PCRs showing the level of *Dilp8* (T) and *Xrp1* (U) mRNAs in wing imaginal discs in which NOC1 and Eiger levels were reduced using the *rotund-Gal4* promoter; *actin5C* mRNA was used as control. Data are mean±s.d. for three experiments. (X) Model: NOC1 is necessary for proper rRNA processing. Its reduction decreases protein synthesis and induces a nucleolar stress resulting in apoptosis. This event is accompanied by the upregulation of the pro-apoptotic genes *eiger* and Xrp1, resulting in DILP8 upregulation that in turn reduces ecdysone delaying animal development. **P*<0.05; ***P*<0.01; ****P*<0.001; *****P*<0.0001; ns, not significant (one-way ANOVA with Tukey multiple comparisons). Scale bars: 40 µm (A–C); 1 mm (F–H); 100 µm (I-L; N–Q;R,S,V,W).

competition. We also showed the relevance of NOC1 in promoting nucleolar stress and apoptosis, both leading cause of tumor formation (Penzo et al., 2019; Quin et al., 2014). Our data support a potential role for the human homolog CEBPz in the context of tumorigenesis. Indeed, mutations in CEBPz are described in >1.5% of tumors of epithelial origins (cBioPortal; https://www.cbioportal.org/results/cancerTypesSummary?cancer_study_list=pancan_pcawg_2020&Z_SCORE_THRESHOLD=2.0&RPPA_SCORE_THRESHOLD=2.0&profileFilter=mutations%>2Ccna&case_set_id=pancan_pcawg_2020_cnaseq&gene_list=CEBPZ&geneset_list=%20&tab_index=tab_visualize&Action=Submit), suggesting that it might have a role in contributing to the signals

Journal of Cell Science (2022) 135, jcs260110. doi:10.1242/jcs.260110

that trigger proteotoxic stress associated to tumorigenesis (Mills and Green, 2017; Narla and Ebert, 2010). CEBPz was also found, together with the METTL3–METTL14 methyltransferase complex, to control cellular growth (Barbieri et al., 2017) and to have a role in the regulation of H3K9m3 histone methylation in response to sonication-resistant heterochromatin (srHC), highlighting it as a moonlighting protein for RNA and heterochromatin modifications (McCarthy et al., 2021).

MATERIALS AND METHODS

Drosophila husbandry and lines

Animals were raised at low density in vials containing standard fly food, composed of 9 g/l agar, 75 g/l corn flour, 50 g/l fresh yeast, 30 g/l yeast extract, 50 g/l white sugar and 30 ml/l molasses, along with nipagine (in ethanol) and propionic acid. The crosses and flies used for the experiments are kept at 25°C, unless otherwise stated.

The following fly lines were used: *GMR-Gal4* (Parisi et al., 2011), *tub>y+>Gal4; ey-flp* (Bellosta et al., 2005), *P0206-GFP-Gal4* (Valenza et al., 2018), the FB-specific promoter *FB-Gal4* (kind gift from Ines Anderl, University of Tampere, Finland), *rotund-Gal4* and *yw; nubbin>Gal4* (kind gift from Hugo Stocker, ETH Zurich, Switzerland), *actin-Gal4,GFP/Gla,Bla* (a kind gift from Daniela Grifoni University of l'Aquila, Italy), *yw; Actin>CD2>Gal4,GFP/TM6b* (kind gift from Bruce Edgar, University of Boulder, CO, USA), *MS1096-Gal4* (kind gift from Erika Bach, NYU, USA), *Minute(3)66D/+* (Sæboe-Larssen et al., 1997), *engrailed-Gal4* (kind gift from Gary Struhl, Columbia University), *Xrp1-LacZ* (kind gift from Koni Basler, University of Zurich) and *actin-Gal4, GFP; tub-Gal80ts* (originated in this work). The following stocks were obtained from the Bloomington *Drosophila* Stock Center: *Cg-Gal4.A2* (B7011), *elav-Gal4* (B458), *UAS-CG7839-RNAi (B25992)*, *UAS-CG9246-RNAi* (B50907), *UAS-CG1234-RNAi* (B61872), *CG7839-GFP.FTPD* (B51967), *dilp8-GFPMI00727* (B33079), *TRE-dsRedT4* (B59011); and from the Vienna *Drosophila* Resource Center: *UAS-CG7839-RNAi* (v12691), *sgRNA^{CG7839}-CFDlib01132* (v341898), *hh-Gal4;uMCas9* (v340019), *w^{1118}* (v60000), *UAS-eiger-RNAi* (v45253), *eiger-GFP-2XTY1-SGFP-V5-preTEV-BLRP-3XFLAG* (v318615); and from FlyORF (ZH) the line *UAS-CG7839-3xHA* (F001775).

Measurement of larval length and volume

Larvae at the indicated stage of development and genotypes were anesthetized using freezing cold temperature, and pictures were taken using a Leica MZ16F stereomicroscope. Width and length were measured using a grid, and volume was calculated by applying the formula in Parisi et al. (2013).

qRT-PCR

RNA extraction was performed using the RNeasy Mini Kit (Qiagen), following the manufacturer's instructions. The isolated RNA was quantified with the Nanodrop2000. 1000 ng of total RNA were retrotranscribed into cDNA using the SuperScript IV VILO Master Mix (Invitrogen). The obtained cDNA was used for qRT-PCR using the SYBR Green PCR Kit (Qiagen). The assays were performed on a Bio-Rad CFX96 machine and the analysis were done using Bio-Rad CFX Manager software. Transcript abundance was normalized to that of *actin5c*. The list of the primers is available in Table S2.

Dissection and immunofluorescence

Larvae were collected at the third-instar stage, dissected in 1× phosphate-buffered saline (PBS), and fixed for 30 min in 4% paraformaldehyde (PFA) at room temperature (RT). After 15 min of tissue permeabilization with 0.3% Triton X-100, samples were washed in PBS with 0.04% Tween 20 (PBST) and blocked in 1% bovine serum albumin (BSA) for 1 h at RT. Samples were incubated overnight at 4°C with primary antibodies in 1% BSA and, after washing, with Alexa-Fluor-488- or 555-conjugated secondary antibodies at 1:2000 in BSA. During washing in PBST, nuclei were stained with Hoechst 33342 (Thermo Fisher Scientific). Imaginal discs were dissected from the carcasses and mounted on slides with Vectashield (LsBio-Vector Laboratories). Images were acquired using a Leica SP5 and SP8 confocal microscopes and assembled using Photoshop2020 (Adobe). Primary antibodies used were: rat anti-HA, 1:1000 (Roche 3f10); mouse anti-fibrillarin, 1:100 (Abcam ab4566); mouse anti-WG, 1:100 (DSHB 4D4); and rabbit anti-cleaved caspase 3, 1:400 (Cell Signaling 9661). Fluorescence intensity was determined by measuring the mean gray value in the wing pouch with ImageJ software.

Western blotting

Proteins were extracted from third-instar larvae and collected in 250 µl of lysis buffer (50 mM HEPES pH 7.4, 250 mM NaCl, 1 mM EDTA and 1.5% Triton X-100) containing a cocktail of phosphatases and proteases inhibitors (Roche). Samples were run on a SDS-polyacrylamide gel and then transferred to a nitrocellulose membrane. After blocking with 5% non-fat milk in TBST, membranes were incubated with primary antibodies against puromycin (1:1000; clone 12D10 MABE343, Merk), mouse anti-HA (1:200; supernatant Sigma HA7) and anti-actin (1:200; DSHB 224-236-1), followed by incubation with HRP-conjugated secondary antibodies (Santa Cruz Biotechnology), and signal was detected using ECL LiteAblot Plus (Euroclone) and the UVITec Alliance LD2.

SUnSET assay

UAS-NOC1-RNAi was expressed ubiquitously in whole larvae using *actin-Gal4* coupled with the *tubulin-Gal80* temperature-sensitive allele to avoid early lethality. Crosses were kept at 18°C and when larvae reached second instar were switched to 30°C for 72 h prior to dissection. At least seven third-instar larvae for each genotype were dissected in Schneider's medium and then transferred to Eppendorf tubes containing Schneider's medium with 10% serum plus puromycin at 20 µg/ml (Invitrogen, Thermo Fisher Scientific). The samples were incubated for 40 or 60 min at room temperature, then recovered in 10% serum in Schneider's medium without puromycin for 30 min at room temperature. Then, the inverted larvae were snap frozen in liquid nitrogen for subsequent western blot analysis using anti-puromycin primary antibody.

Polysome profiling

Cytoplasmic lysates were obtained from snap-frozen whole larvae pulverized using liquid nitrogen. After addition of lysis buffer and centrifugation (16,000 ***g*** for 30 min) for removal of the debris, cleared supernatants were loaded on a linear 10%–40% sucrose gradient and ultracentrifuged in a SW41Ti rotor (Beckman) for 1 h and 30 min at 270,000 ***g*** at 4°C in a Beckman Optima LE-80K ultracentrifuge. After ultracentrifugation, gradients were fractionated in 1 ml volume fractions with continuous monitoring of absorbance at 254 nm using an ISCO UA-6 UV detector. % of ribosomal subunits was calculated over the (40, 60, 80 and polysome) area of the same genotype.

Generation of inducible flip-out clones and clonal analysis

Females, *yw; Actin>CD2>Gal4-GFP/TM6b* were crossed with males carrying the heat-shock *Flippase y^{122}w* together with the appropriate UAS transgenes. Animals were left laying eggs for 3–4 h. Heat shock was performed on larvae at 48 or 72 h after egg laying (AEL) for 15 min at 37°C. Larvae were dissected at 96 or at 120 h AEL and mounted using MOWIOL. Images of clones expressing nuclear GFP were acquired using a LEICA SP8 confocal microscope. Quantification of the number of GFP-positive cells/clone in the wing imaginal discs was calculated from five confocal images for every genotype at 40× objective magnification maintaining constant acquisition parameters. Co-staining with phalloidin–Rhodamine (Invitrogen) was necessary in Fig. 5A–E to outline the cell membranes and with DAPI for the nuclei.

Imaging the adult compound eye and wings

Photographs of eyes of adult females expressing the indicated UAS transgenes in the retina driven by the *GMR-Gal4* or *tub>y+>Gal4* promoters were taken at 8 days after eclosion using a Leica stereomicroscope MZ16F at 4× magnification. To analyze wings, 2–4-day-old animals were fixed in a solution of 1:1 glycerol and ethanol. One

wing was dissected from at least 10 animals and mounted on a slide in the same fixing solution. Images of each wing were taken using a Zeiss Axio Imager M2 microscope with a 1× objective magnification. Quantification of the area of each wing and eye was performed on photographs using Photoshop.

Fat body staining and cell size calculation

FBs were dissected from larvae at 5 or 12 days AEL fixed in 4% PFA and counterstained with Nile Red (Sigma), phalloidin-488 (Invitrogen) and Hoechst 33258 (Sigma). After washing with PBS, FBs were mounted onto slides with DABCO-Mowiol (Sigma-Aldrich) and images were acquired using the LeicaSP5-LEICA microscope; the area of adipose cells for each FB was calculated with ImageJ software. Measurement of TGA levels and visualization of lipids in the whole larvae was performed as in Parisi et al. (2013) using Nile Red staining. Dissected organs were mounted in DABCO-Mowiol and photographs were taken using a Zeiss Axio M2 Imager light microscope.

Generation of CRISPR-Cas9 mutations of *NOC1*/*CG7839* and analysis of their function in the posterior compartment of wing imaginal disc

To target mutations in CG7839 into the germ line we crossed the line nos-Gal4VP16 UAS-uMCas9(attP40) with gRNA line for *CG7839* (*vCFDlib01132*) from the Boutros collection (Port et al., 2020). Out of 30 putative lines carrying potential NOC1 heterozygous mutations, we sequenced five lines and two of them contained indels that create nonsense mutations that led to *NOC1* mRNAs being translated into short NOC1 polypeptidic sequences of 30 amino acids (NOC1-mut^{12}) and 29 amino acids (NOC1-mut^{14}). Sequences of the primers used for the screening are in Table S2. Phenotypic analysis of NOC1-mutant homozygous larvae was carried by leaving heterozygous *w*^{1118}*; NOC1-mutant/TM6b* parents to lay eggs for 5 h at 25°C in regular food. Homozygous (not *tubby*) larvae were scored, and pictures were taken at 8 days AEL. At this stage, heterozygous *NOC1/TM6b* larvae were the only pupae that hatched at the expected time. Mutations of *CG7938* were targeted in the posterior compartment of the wing imaginal disc by using the line *UAS-uMCas9; hh-Gal4/TM6B* to spatially limit the transcription of Cas9 in the posterior region of the animal under *hh-Gal4* (Port et al., 2020). This line was crossed with that carrying the sgRNA for *CG7839* (*vCFDlib01132*) previously recombined with *UAS-GFP* to mark the posterior compartment. A line expressing only *UAS-GFP* was used as control. F1 animals were dissected at ∼90 h AEL and images of their wing imaginal discs were acquired using a confocal microscope (Leica SP8). Calculation of the size of the posterior compartment (GFP positive) and the total area of the wing imaginal discs were performed using Adobe Photoshop. At least eight animals from each genotype were used for the statistical analysis.

Statistical analysis

Unpaired two-tailed Student's *t*-test analysis and one-way ANOVA with Tukey multi-comparisons analyses were performed using GraphPad-PRISM*8*. *P*-values are indicated with asterisks (*P<0.05, **P<0.01, ***P<0.001, ****P<0.0001).

Acknowledgements

We thank Marcello Ceci for reading the manuscript and for the useful discussion, the Advanced Imaging Core Facility at CIBIO, the Vienna VDRC and Bloomington Stock Centers and the DSHB for antibodies. Stocks obtained from the Bloomington Drosophila Stock Center (NIH P40OD018537) were used in this study. We apologize in advance to any authors whose work has been omitted. Department CIBIO Core Facilities are supported by the European Regional Development Fund (ERDF) 2014–2020.

Competing interests

The authors declare no competing or financial interests.

Author contributions

Conceptualization: F.D., V.M., S.S., S.Z., M.B., G. Viola, P.M., P.B.; Formal analysis: F.D., V.M., S.S., S.Z., M.B., G. Viola, P.M., G. Viero, M.E.P., P.B.; Data curation: F.D., V.M., S.S., S.Z., M.B., G. Viola, P.M., I.S., G. Viero, M.E.P., M.P., P.B.; Writing - original draft: F.D., V.M., S.S., P.B.; Writing - review & editing: F.D., V.M., S.S., S.Z., G. Viola, G. Viero, M.P., P.B.; Supervision: P.B.; Funding acquisition: M.E.P., P.B.

Funding

This work was supported by an National Institutes of Health (NIH) Public Health Service grant from the NIH-SC1DK085047 to P.B. and S.Z., and MAE PGR00155 to M.E.P. Deposited in PMC for release after 12 months.

Peer review history

The peer review history is available online at https://journals.biologists.com/jcs/lookup/doi/10.1242/jcs.260110.reviewer-comments.pdf

References

Akai, N., Ohsawa, S., Sando, Y. and Igaki, T. (2021). Epithelial cell-turnover ensures robust coordination of tissue growth in Drosophila ribosomal protein mutants. *PLoS Genet.* **17**, e1009300. doi:10.1371/journal.pgen.1009300

Andersen, D. S., Colombani, J. and Léopold, P. (2013). Coordination of organ growth: principles and outstanding questions from the world of insects. *Trends Cell Biol.* **23**, 336-344. doi:10.1016/j.tcb.2013.03.005

Baillon, L., Germani, F., Rockel, C., Hilchenbach, J. and Basler, K. (2018). Xrp1 is a transcription factor required for cell competition-driven elimination of loser cells. *Sci. Rep.* **8**, 17712. doi:10.1038/s41598-018-36277-4

Baker, N. E. (2020). Emerging mechanisms of cell competition. *Nat. Rev. Genet.* **21**, 683-697. doi:10.1038/s41576-020-0262-8

Baral, S. S., Lieux, M. E. and Dimario, P. J. (2020). Nucleolar stress in Drosophila neuroblasts, a model for human ribosomopathies. *Biol. Open* **9**, bio046565. doi:10.1242/bio.046565

Barbieri, I., Tzelepis, K., Pandolfini, L., Shi, J., Millan-Zambrano, G., Robson, S. C., Aspris, D., Migliori, V., Bannister, A. J., Han, N. et al. (2017). Promoter-bound METTL3 maintains myeloid leukaemia by m(6)A-dependent translation control. *Nature* **552**, 126-131. doi:10.1038/nature24678

Barna, M., Pusic, A., Zollo, O., Costa, M., Kondrashov, N., Rego, E., Rao, P. H. and Ruggero, D. (2008). Suppression of Myc oncogenic activity by ribosomal protein haploinsufficiency. *Nature* **456**, 971-975. doi:10.1038/nature07449

Baumgartner, M. E., Dinan, M. P., Langton, P. F., Kucinski, I. and Piddini, E. (2021). Proteotoxic stress is a driver of the loser status and cell competition. *Nat. Cell Biol.* **23**, 136-146. doi:10.1038/s41556-020-00627-0

Bellosta, P., Hulf, T., Balla Diop, S., Usseglio, F., Pradel, J., Aragnol, D. and Gallant, P. (2005). Myc interacts genetically with Tip48/Reptin and Tip49/Pontin to control growth and proliferation during Drosophila development. *Proc. Natl. Acad. Sci. USA* **102**, 11799-11804. doi:10.1073/pnas.0408945102

Boulan, L. and Léopold, P. (2021). What determines organ size during development and regeneration? *Development* **148**, dev196063. doi:10.1242/dev.196063

Brown, B., Mitra, S., Roach, F. D., Vasudevan, D. and Ryoo, H. D. (2021). The transcription factor Xrp1 is required for PERK-mediated antioxidant gene induction in Drosophila. *Elife* **10**, e74047. doi:10.7554/eLife.74047

Capdevila, J. and Guerrero, I. (1994). Targeted expression of the signaling molecule decapentaplegic induces pattern duplications and growth alterations in Drosophila wings. *EMBO J.* **13**, 4459-4468. doi:10.1002/j.1460-2075.1994.tb06768.x

Deliu, L. P., Ghosh, A. and Grewal, S. S. (2017). Investigation of protein synthesis in Drosophila larvae using puromycin labelling. *Biol. Open* **6**, 1229-1234. doi:10.1242/bio.026294

Destefanis, F., Manara, V. and Bellosta, P. (2020). Myc as a regulator of ribosome biogenesis and cell competition: a link to cancer. *Int. J. Mol. Sci.* **21**, 4037. doi:10.3390/ijms21114037

Edskes, H. K., Ohtake, Y. and Wickner, R. B. (1998). Mak21p of Saccharomyces cerevisiae, a homolog of human CAATT-binding protein, is essential for 60 S ribosomal subunit biogenesis. *J. Biol. Chem.* **273**, 28912-28920. doi:10.1074/jbc.273.44.28912

Garelli, A., Heredia, F., Casimiro, A. P., Macedo, A., Nunes, C., Garcez, M., Dias, A. R., Volonte, Y. A., Uhlmann, T., Caparros, E. et al. (2015). Dilp8 requires the neuronal relaxin receptor Lgr3 to couple growth to developmental timing. *Nat. Commun.* **6**, 8732. doi:10.1038/ncomms9732

Géminard, C., Rulifson, E. J. and Léopold, P. (2009). Remote control of insulin secretion by fat cells in Drosophila. *Cell Metab.* **10**, 199-207. doi:10.1016/j.cmet.2009.08.002

Grewal, S. S., Li, L., Orian, A., Eisenman, R. N. and Edgar, B. A. (2005). Myc-dependent regulation of ribosomal RNA synthesis during Drosophila development. *Nat. Cell Biol.* **7**, 295-302. doi:10.1038/ncb1223

Hay, B. A., Wolff, T. and Rubin, G. M. (1994). Expression of baculovirus P35 prevents cell death in Drosophila. *Development* **120**, 2121-2129. doi:10.1242/dev.120.8.2121

Herold, T., Metzeler, K. H., Vosberg, S., Hartmann, L., Rollig, C., Stolzel, F., Schneider, S., Hubmann, M., Zellmeier, E., Ksienzyk, B. et al. (2014). Isolated trisomy 13 defines a homogeneous AML subgroup with high frequency of

mutations in spliceosome genes and poor prognosis. *Blood* **124**, 1304-1311. doi:10.1182/blood-2013-12-540716

Hierlmeier, T., Merl, J., Sauert, M., Perez-Fernandez, J., Schultz, P., Bruckmann, A., Hamperl, S., Ohmayer, U., Rachel, R., Jacob, A. et al. (2013). Rrp5p, Noc1p and Noc2p form a protein module which is part of early large ribosomal subunit precursors in S. cerevisiae. *Nucleic Acids Res.* **41**, 1191-1210. doi:10.1093/nar/gks1056

Hironaka, K. I., Fujimoto, K. and Nishimura, T. (2019). Optimal scaling of critical size for metamorphosis in the genus Drosophila. *iScience* **20**, 348-358. doi:10.1016/j.isci.2019.09.033

Horng, T. and Hotamisligil, G. S. (2011). Linking the inflammasome to obesity-related disease. *Nat. Med.* **17**, 164-165. doi:10.1038/nm0211-164

Hyun, S. (2018). Body size regulation by maturation steroid hormones: a Drosophila perspective. *Front. Zool.* **15**, 44. doi:10.1186/s12983-018-0290-9

Ji, Z., Kiparaki, M., Folgado, V., Kumar, A., Blanco, J., Rimesso, G., Chuen, J., Liu, Y., Zheng, D. and Baker, N. E. (2019). Drosophila RpS12 controls translation, growth, and cell competition through Xrp1. *PLoS Genet.* **15**, e1008513. doi:10.1371/journal.pgen.1008513

Johnston, L. A., Prober, D. A., Edgar, B. A., Eisenman, R. N. and Gallant, P. (1999). Drosophila myc regulates cellular growth during development. *Cell* **98**, 779-790. doi:10.1016/S0092-8674(00)81512-3

Khoshnevis, S., Liu, X., Dattolo, M. D. and Karbstein, K. (2019). Rrp5 establishes a checkpoint for 60S assembly during 40S maturation. *RNA* **25**, 1164-1176. doi:10.1261/rna.071225.119

Kiparaki, M., Khan, C., Folgado-Marco, V., Chuen, J., Moulos, P. and Baker, N. E. (2022). The transcription factor Xrp1 orchestrates both reduced translation and cell competition upon defective ribosome assembly or function. *Elife* **11**, e71705. doi:10.7554/eLife.71705

Koyama, T., Texada, M. J., Halberg, K. A. and Rewitz, K. (2020). Metabolism and growth adaptation to environmental conditions in Drosophila. *Cell. Mol. Life Sci.* **77**, 4523-4551. doi:10.1007/s00018-020-03547-2

Kucinski, I., Dinan, M., Kolahgar, G. and Piddini, E. (2017). Chronic activation of JNK JAK/STAT and oxidative stress signalling causes the loser cell status. *Nat. Commun.* **8**, 136. doi:10.1038/s41467-017-00145-y

Kudron, M. M., Victorsen, A., Gevirtzman, L., Hillier, L. W., Fisher, W. W., Vafeados, D., Kirkey, M., Hammonds, A. S., Gersch, J., Ammouri, H. et al. (2018). The ModERN resource: genome-wide binding profiles for hundreds of Drosophila and Caenorhabditis elegans transcription factors. *Genetics* **208**, 937-949. doi:10.1534/genetics.117.300657

Langton, P. F., Baumgartner, M. E., Logeay, R. and Piddini, E. (2021). Xrp1 and Irbp18 trigger a feed-forward loop of proteotoxic stress to induce the loser status. *PLoS Genet.* **17**, e1009946. doi:10.1371/journal.pgen.1009946

Lee, C. H., Kiparaki, M., Blanco, J., Folgado, V., Ji, Z., Kumar, A., Rimesso, G. and Baker, N. E. (2018). A regulatory response to ribosomal protein mutations controls translation, growth, and cell competition. *Dev. Cell* **46**, 456-469.e4. doi:10.1016/j.devcel.2018.07.003

Li, N., Yuan, L., Liu, N., Shi, D., Li, X., Tang, Z., Liu, J., Sundaresan, V. and Yang, W. C. (2009). SLOW WALKER2, a NOC1/MAK21 homologue, is essential for coordinated cell cycle progression during female gametophyte development in Arabidopsis. *Plant Physiol.* **151**, 1486-1497. doi:10.1104/pp.109.142414

Liu, Y., Mattila, J., Ventelä, S., Yadav, L., Zhang, W., Lamichane, N., Sundström, J., Kauko, O., Grénman, R., Varjosalo, M. et al. (2017). PWP1 mediates nutrient-dependent growth control through nucleolar regulation of ribosomal gene expression. *Dev. Cell* **43**, 240-252.e5. doi:10.1016/j.devcel.2017.09.022

Lum, L. S., Sultzman, L. A., Kaufman, R. J., Linzer, D. I. and Wu, B. J. (1990). A cloned human CCAAT-box-binding factor stimulates transcription from the human hsp70 promoter. *Mol. Cell. Biol.* **10**, 6709-6717. doi:10.1128/mcb.10.12.6709-6717.1990

Maniere, G., Alves, G., Berthelot-Grosjean, M. and Grosjean, Y. (2020). Growth regulation by amino acid transporters in Drosophila larvae. *Cell. Mol. Life Sci.* **77**, 4289-4297. doi:10.1007/s00018-020-03535-6

Marygold, S. J., Roote, J., Reuter, G., Lambertsson, A., Ashburner, M., Millburn, G. H., Harrison, P. M., Yu, Z., Kenmochi, N., Kaufman, T. C. et al. (2007). The ribosomal protein genes and Minute loci of Drosophila melanogaster. *Genome Biol.* **8**, R216. doi:10.1186/gb-2007-8-10-r216

Mccarthy, R. L., Kaeding, K. E., Keller, S. H., Zhong, Y., Xu, L., Hsieh, A., Hou, Y., Donahue, G., Becker, J. S., Alberto, O. et al. (2021). Diverse heterochromatin-associated proteins repress distinct classes of genes and repetitive elements. *Nat. Cell Biol.* **23**, 905-914. doi:10.1038/s41556-021-00725-7

Milkereit, P., Gadal, O., Podtelejnikov, A., Trumtel, S., Gas, N., Petfalski, E., Tollervey, D., Mann, M., Hurt, E. and Tschochner, H. (2001). Maturation and intranuclear transport of pre-ribosomes requires Noc proteins. *Cell* **105**, 499-509. doi:10.1016/S0092-8674(01)00358-0

Mills, E. W. and Green, R. (2017). Ribosomopathies: there's strength in numbers. *Science* **358**, eaan2755. doi:10.1126/science.aan2755

Narla, A. and Ebert, B. L. (2010). Ribosomopathies: human disorders of ribosome dysfunction. *Blood* **115**, 3196-3205. doi:10.1182/blood-2009-10-178129

Neumuller, R. A., Gross, T., Samsonova, A. A., Vinayagam, A., Buckner, M., Founk, K., Hu, Y., Sharifpoor, S., Rosebrock, A. P., Andrews, B. et al. (2013). Conserved regulators of nucleolar size revealed by global phenotypic analyses. *Sci. Signal.* **6**, ra70. doi:10.1126/scisignal.2004145

Nijhout, H. F., Riddiford, L. M., Mirth, C., Shingleton, A. W., Suzuki, Y. and Callier, V. (2014). The developmental control of size in insects. *Wiley Interdiscip. Rev. Dev. Biol.* **3**, 113-134. doi:10.1002/wdev.124

Palm, W., Sampaio, J. L., Brankatschk, M., Carvalho, M., Mahmoud, A., Shevchenko, A. and Eaton, S. (2012). Lipoproteins in Drosophila melanogaster–assembly, function, and influence on tissue lipid composition. *PLoS Genet.* **8**, e1002828. doi:10.1371/journal.pgen.1002828

Parisi, F., Riccardo, S., Daniel, M., Saqcena, M., Kundu, N., Pession, A., Grifoni, D., Stocker, H., Tabak, E. and Bellosta, P. (2011). Drosophila insulin and target of rapamycin (TOR) pathways regulate GSK3 beta activity to control Myc stability and determine Myc expression in vivo. *BMC Biol.* **9**, 65. doi:10.1186/1741-7007-9-65

Parisi, F., Riccardo, S., Zola, S., Lora, C., Grifoni, D., Brown, L. M. and Bellosta, P. (2013). dMyc expression in the fat body affects DILP2 release and increases the expression of the fat desaturase Desat1 resulting in organismal growth. *Dev. Biol.* **379**, 64-75. doi:10.1016/j.ydbio.2013.04.008

Penzo, M., Montanaro, L., Trere, D. and Derenzini, M. (2019). The ribosome biogenesis-cancer connection. *Cells* **8**, 55. doi:10.3390/cells8010055

Pirillo, A., Casula, M., Olmastroni, E., Norata, G. D. and Catapano, A. L. (2021). Global epidemiology of dyslipidaemias. *Nat. Rev. Cardiol.* **18**, 689-700. doi:10.1038/s41569-021-00541-4

Port, F., Strein, C., Stricker, M., Rauscher, B., Heigwer, F., Zhou, J., Beyersdorffer, C., Frei, J., Hess, A., Kern, K. et al. (2020). A large-scale resource for tissue-specific CRISPR mutagenesis in Drosophila. *Elife* **9**, e53865. doi:10.7554/eLife.53865

Quin, J. E., Devlin, J. R., Cameron, D., Hannan, K. M., Pearson, R. B. and Hannan, R. D. (2014). Targeting the nucleolus for cancer intervention. *Biochim. Biophys. Acta* **1842**, 802-816. doi:10.1016/j.bbadis.2013.12.009

Rusten, T. E., Lindmo, K., Juhasz, G., Sass, M., Seglen, P. O., Brech, A. and Stenmark, H. (2004). Programmed autophagy in the Drosophila fat body is induced by ecdysone through regulation of the PI3K pathway. *Dev. Cell* **7**, 179-192. doi:10.1016/j.devcel.2004.07.005

Sæboe-Larssen, S., Urbanczyk Mohebi, B. and Lambertsson, A. (1997). The Drosophila ribosomal protein L14-encoding gene, identified by a novel Minute mutation in a dense cluster of previously undescribed genes in cytogenetic region 66D. *Mol. Gen. Genet.* **255**, 141-151. doi:10.1007/s004380050482

Sæboe-Larssen, S., Lyamouri, M., Merriam, J., Oksvold, M. P. and Lambertsson, A. (1998). Ribosomal protein insufficiency and the minute syndrome in Drosophila: a dose-response relationship. *Genetics* **148**, 1215-1224. doi:10.1093/genetics/148.3.1215

Sanchez, J. A., Mesquita, D., Ingaramo, M. C., Ariel, F., Milán, M. and Dekanty, A. (2019). Eiger/TNFα-mediated Dilp8 and ROS production coordinate intra-organ growth in Drosophila. *PLoS Genet.* **15**, e1008133. doi:10.1371/journal.pgen.1008133

Schmid, M. R., Anderl, I., Vesala, L., Vanha-Aho, L. M., Deng, X. J., Rämet, M. and Hultmark, D. (2014). Control of Drosophila blood cell activation via Toll signaling in the fat body. *PLoS One* **9**, e102568. doi:10.1371/journal.pone.0102568

Scott, R. C., Schuldiner, O. and Neufeld, T. P. (2004). Role and regulation of starvation-induced autophagy in the Drosophila fat body. *Dev. Cell* **7**, 167-178. doi:10.1016/j.devcel.2004.07.009

Shokri, L., Inukai, S., Hafner, A., Weinand, K., Hens, K., Vedenko, A., Gisselbrecht, S. S., Dainese, R., Bischof, J., Furger, E. et al. (2019). A comprehensive Drosophila melanogaster transcription factor interactome. *Cell Rep.* **27**, 955-970.e7. doi:10.1016/j.celrep.2019.03.071

Texada, M. J., Koyama, T. and Rewitz, K. (2020). Regulation of body size and growth control. *Genetics* **216**, 269-313. doi:10.1534/genetics.120.303095

Tortoriello, G., De Celis, J. F. and Furia, M. (2010). Linking pseudouridine synthases to growth, development and cell competition. *FEBS J.* **277**, 3249-3263. doi:10.1111/j.1742-4658.2010.07731.x

Valenza, A., Bonfanti, C., Pasini, M. E. and Bellosta, P. (2018). Anthocyanins function as anti-inflammatory agents in a Drosophila model for adipose tissue macrophage infiltration. *Biomed. Res. Int.* **2018**, 6413172. doi:10.1155/2018/6413172

Vallejo, D. M., Juarez-Carreno, S., Bolivar, J., Morante, J. and Dominguez, M. (2015). A brain circuit that synchronizes growth and maturation revealed through Dilp8 binding to Lgr3. *Science* **350**, aac6767. doi:10.1126/science.aac6767

Van Riggelen, J., Yetil, A. and Felsher, D. W. (2010). MYC as a regulator of ribosome biogenesis and protein synthesis. *Nat. Rev. Cancer* **10**, 301-309. doi:10.1038/nrc2819